White Rose Research Online

eprints@whiterose.ac.uk
https://eprints.whiterose.ac.uk
Universities of Leeds, Sheffield and York

Deposited via The University of Sheffield.

White Rose Research Online URL for this paper:
https://eprints.whiterose.ac.uk/id/eprint/201383/

Version: Published Version

Article:
Aad, G., Abbott, B., Abbott, D.C. et al. (2023) Measurement of the CP properties of Higgs boson interactions with τ -leptons with the ATLAS detector. The European Physical Journal C, 83 (7). 563. ISSN: 1434-6044

https://doi.org/10.1140/epjc/s10052-023-11583-y

Reuse
This article is distributed under the terms of the Creative Commons Attribution (CC BY) licence. This licence allows you to distribute, remix, tweak, and build upon the work, even commercially, as long as you credit the authors for the original work. More information and the full terms of the licence here:
https://creativecommons.org/licenses/

Takedown
If you consider content in White Rose Research Online to be in breach of UK law, please notify us by emailing eprints@whiterose.ac.uk including the URL of the record and the reason for the withdrawal request.

UNIVERSITY OF LEEDS
University of Sheffield
UNIVERSITY of York

Eur. Phys. J. C (2023) 83:563
https://doi.org/10.1140/epjc/s10052-023-11583-y

THE EUROPEAN PHYSICAL JOURNAL C

Regular Article - Experimental Physics

Measurement of the *CP* properties of Higgs boson interactions with τ-leptons with the ATLAS detector

ATLAS Collaboration[⋆]

CERN, 1211 Geneva 23, Switzerland

Received: 13 December 2022 / Accepted: 27 January 2023
© CERN for the benefit of the ATLAS collaboration 2023

Abstract A study of the charge conjugation and parity (*CP*) properties of the interaction between the Higgs boson and τ-leptons is presented. The study is based on a measurement of *CP*-sensitive angular observables defined by the visible decay products of τ-leptons produced in Higgs boson decays. The analysis uses 139 fb^{-1} of proton–proton collision data recorded at a centre-of-mass energy of $\sqrt{s} =$ 13 TeV with the ATLAS detector at the Large Hadron Collider. Contributions from *CP*-violating interactions between the Higgs boson and τ-leptons are described by a single mixing angle parameter ϕ_τ in the generalised Yukawa interaction. Without constraining the $H \to \tau\tau$ signal strength to its expected value under the Standard Model hypothesis, the mixing angle ϕ_τ is measured to be $9° \pm 16°$, with an expected value of $0° \pm 28°$ at the 68% confidence level. The pure *CP*-odd hypothesis is disfavoured at a level of 3.4 standard deviations. The results are compatible with the predictions for the Higgs boson in the Standard Model.

1 Introduction

A detailed analysis of Higgs boson (H) decays into τ-lepton pairs observed at the LHC [1–3] allows a direct probe of the charge conjugation and parity (*CP*) properties of the Yukawa coupling of the Higgs boson to the τ-lepton. The Standard Model (SM) of particle physics predicts the Higgs boson to be a *CP*-even (scalar) particle. The presence of a *CP*-odd (pseudoscalar) admixture has not yet been excluded, and any observed *CP*-odd contribution to the $H\tau\tau$ coupling properties would be a sign of physics beyond the SM.

Studies of the *CP* properties of Higgs boson interactions with gauge bosons performed by the ATLAS and CMS experiments [4–9] have shown no deviation from the SM predictions. However, these measurements probe the bosonic couplings in which *CP*-odd contributions enter only via higher-order operators that are suppressed by powers of $1/\Lambda^2$ [10], where Λ is the scale of the new physics in an effective field theory. In contrast, a *CP*-odd contribution to Yukawa couplings can be present at tree level. Recently, measurements of the *CP* properties of the interaction between the Higgs boson and top quarks were performed by the ATLAS [11] and CMS [12] Collaborations, and excluded a pure *CP*-odd structure for the top-quark Yukawa coupling at 3.9σ and 3.2σ, respectively.

This paper presents a measurement of the *CP* properties of the Higgs boson interaction with τ-leptons. The measurement is based on *CP*-sensitive angular observables defined using the visible τ-lepton decay products. Ideas about how to probe a *CP*-odd and *CP*-even admixture in the τ-lepton Yukawa coupling in $H \to \tau\tau$ decay were initially developed in the context of e^+e^- colliders [13–17]. Originally, hadronic decays of the τ-leptons into $\pi^\pm\nu$ and $\rho^\pm\nu$ were used, and observables sensitive to the transverse spin correlations between the τ-lepton decay products were constructed. These methods, extended to $\ell^\pm(= e^\pm, \mu^\pm)\nu\nu$ and $a_1^\pm\nu$ decays and re-evaluated in the context of pp collisions at the LHC [18–23], are adopted in this analysis. Recently, a similar study was also performed by the CMS Collaboration [24].

The general effective Yukawa interaction between the Higgs boson and τ-leptons can be parameterised as in Refs. [21,23]:

$$\mathcal{L}_{H\tau\tau} = -\frac{m_\tau}{\upsilon}\kappa_\tau(\cos\phi_\tau\bar{\tau}\tau + \sin\phi_\tau\bar{\tau}i\gamma_5\tau)H,$$

where $\upsilon = 246$ GeV is the vacuum expectation value of the Higgs field, κ_τ is the reduced Yukawa coupling strength, and ϕ_τ (where $\phi_\tau \in [-90°, 90°]$) is the *CP*-mixing angle that parameterises the relative contributions of the *CP*-even and *CP*-odd components to the $H\tau\tau$ coupling. The SM *CP*-even hypothesis is realised for $\phi_\tau = 0°$, while the pure *CP*-odd scenario corresponds to $\phi_\tau = \pm 90°$. Other values of ϕ_τ represent admixtures of the two components and would indicate a *CP*-violating scenario.

The *CP*-mixing angle ϕ_τ is encoded in the correlations between the transverse spin components of the τ-leptons in the $H \to \tau\tau$ decays, which are then reflected in the direc-

⋆ e-mail: atlas.publications@cern.ch

Published online: 04 July 2023

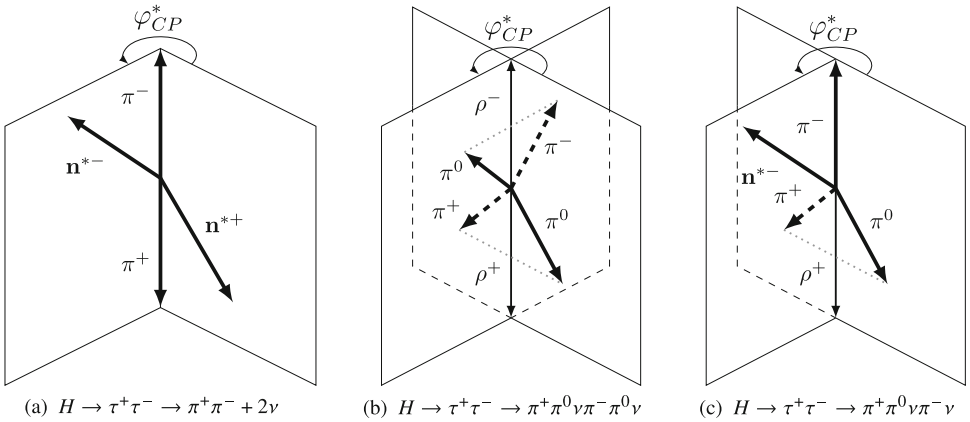

Fig. 1 Illustration of the τ-lepton decay planes for constructing the φ^*_{CP} observable in **a** $H \to \tau^+\tau^- \to \pi^+\pi^- + 2\nu$ decay using the impact parameter method, **b** $H \to \tau^+\tau^- \to \pi^+\pi^0\nu\pi^-\pi^0\nu$ using the ρ-decay plane method, and **c** $H \to \tau^+\tau^- \to \pi^+\pi^0\nu\pi^-\nu$ using the combined impact parameter and ρ-decay plane method. The decay planes are spanned by the spatial momentum vector of the charged decay particle of the τ-lepton ($\pi^\pm$) and either its impact parameter $\mathbf{n}^{*\pm}$ or the spatial momentum vector of the neutral decay particle of the τ-lepton (π^0)

tions of the τ-lepton decay products. The signed acoplanarity angle φ^*_{CP} between the τ decay planes (described in Sect. 3 and illustrated in Fig. 1) is sensitive to the transverse spin correlations impacted by the *CP*-mixing angle of the Yukawa coupling. Such correlations are usually calculated by contracting the polarimeter vectors of the decayed τ-leptons[1] and the spin density matrix of the τ-lepton-pair spin state, $R_{i,j}$, which depends on the τ-lepton pair-production process [26–28]. In the case of Higgs boson decays, the spin density matrix $R_{i,j}$ has only transverse components with respect to the τ-lepton direction, and these are first-order trigonometric polynomials in the $2\phi_\tau$ angle. Per-event sensitivity to *CP*-mixing depends on the τ-lepton-pair decay modes and on the way in which the polarimeter vectors and decay planes are reconstructed from observable quantities. The φ^*_{CP} angle is directly related to ϕ_τ in the $H \to \tau\tau$ differential decay rate and the relation has the form of a first-order trigonometric polynomial in $\cos(\varphi^*_{CP} - 2\phi_\tau)$ at leading order [14,21,22]:

$$d\Gamma_{H\to\tau^+\tau^-} \approx 1 - b(E_+)b(E_-)\frac{\pi^2}{16}\cos(\varphi^*_{CP} - 2\phi_\tau),$$

where $E_\pm$ are the energies of the charged decay particles in their respective τ-lepton rest frames, and $b(E_\pm)$ are the spectral functions [29] describing the spin analysing power of a given decay mode. Different methods [15–23] have been developed in an attempt to approximately reconstruct τ-lepton decay planes. The φ^*_{CP} variable used in this analysis is constructed with various methods depending on the τ-lepton decay modes, largely following the strategy presented in Ref. [23].

The analysis is performed using 139 fb^{-1} of $\sqrt{s} = 13$ TeV proton–proton (pp) collision data recorded from 2015 to 2018 with the ATLAS detector. Two τ-lepton-pair decay channels are considered in the analysis: the first with one leptonically (τ_{lep}) and one hadronically decaying τ-lepton (τ_{had}), referred to as the $\tau_{\text{lep}}\,\tau_{\text{had}}$ channel, and the second with two hadronically decaying τ-leptons, referred to as the $\tau_{\text{had}}\,\tau_{\text{had}}$ channel. The leptonic decay $\tau^\pm \to \ell^\pm\nu\nu$ includes decays to either an electron or a muon. In the case of hadronic decay, the dominant τ_{had} decay modes are considered: single-pion decay $\pi^\pm\nu$, two-pion decay $\pi^\pm\pi^0\nu$ with an intermediate $\rho^\pm$, and three-pion decay $\pi^\pm 2\pi^0\nu$ and $3\pi^\pm\nu$ with an intermediate $a_1^\pm$. A small fraction of events with τ decays to $K^\pm$ mesons is also included in the analysis. The τ-lepton decay modes used in the analysis are summarised in Table 1 with their branching fractions [30] and the notation used throughout this paper. The τ_{had} decay modes are labelled by YpXn in accord with the number of charged (Y) and neutral (X) pions among the decay products. The τ-lepton-pair decay modes considered in this analysis account for 68% of all possible τ pair decays.

This paper is structured as follows. In Sect. 2 the ATLAS detector is briefly described. The methodology and observables used in the analysis are discussed in Sect. 3. Section 4 gives a summary of the data and simulated event samples. Section 5 describes the object reconstruction and event selection, and defines the signal and control regions. Section 6 details the experimental and theoretical systematic uncertainties. The fit model and statistical analysis strategy are explained in Sect. 7. Section 8 presents the measurement results. Section 9 concludes the paper.

[1] A polarimeter vector is calculated from the matrix element of the τ-lepton decay process and is usually expressed in terms of the momenta of the decay products. Its direction gives the most probable direction of the τ polarization vector, while its magnitude determines the efficiency of a given decay as a polarimeter [25].

Table 1 Notation for the dominant leptonic and hadronic τ-lepton decay modes used and their branching fractions. The symbol '$\ell^{\pm}$' stands for $e^{\pm}$ or $\mu^{\pm}$, and '$h^{\pm}$' includes $\pi^{\pm}$ and $K^{\pm}$. The parentheses show the hadronic decays involving $\pi^{\pm}$ and their corresponding branching fractions

Notation	Decay mode	Branching fraction
ℓ	$\ell^{\pm}\bar{\nu}\nu$	35.2%
1p0n	$h^{\pm}\nu$ ($\pi^{\pm}\nu$)	11.5% (10.8%)
1p1n	$h^{\pm}\pi^0\nu$ ($\pi^{\pm}\pi^0\nu$)	25.9% (25.5%)
1pXn	$h^{\pm} \geq 2\pi^0\nu$ ($\pi^{\pm}2\pi^0\nu$)	10.8% (9.3%)
3p0n	$3h^{\pm}\nu$ ($3\pi^{\pm}\nu$)	9.8% (9.0%)

2 ATLAS detector

The ATLAS detector [31] at the LHC covers nearly the entire solid angle around the collision point.[2]

It consists of an inner tracking detector surrounded by a thin superconducting solenoid, electromagnetic and hadron calorimeters, and a muon spectrometer incorporating three large superconducting air-core toroidal magnets.

The inner-detector system (ID) is immersed in a 2 T axial magnetic field and provides charged-particle tracking in the range $|\eta| < 2.5$. The high-granularity silicon pixel detector covers the vertex region and typically provides four measurements per track, the first hit normally being in the insertable B-layer [32,33] installed before Run 2. It is followed by the silicon microstrip tracker, which usually provides eight measurements per track. These silicon detectors are complemented by the transition radiation tracker (TRT), which enables radially extended track reconstruction up to $|\eta| = 2.0$. The TRT also provides electron identification information based on the fraction of hits (typically 30 in total) above a higher energy-deposit threshold corresponding to transition radiation.

The calorimeter system covers the pseudorapidity range $|\eta| < 4.9$. Within the region $|\eta| < 3.2$, electromagnetic calorimetry is provided by barrel and endcap high-granularity lead/liquid-argon (LAr) calorimeters, with an additional thin LAr presampler covering $|\eta| < 1.8$ to correct for energy loss in material upstream of the calorimeters. Hadron calorimetry is provided by the steel/scintillator-tile calorimeter, segmented into three barrel structures within $|\eta| < 1.7$, and two copper/LAr hadron endcap calorimeters. The solid angle coverage is completed with forward copper/LAr and tungsten/LAr calorimeter modules optimised for electromagnetic and hadronic energy measurements respectively.

The muon spectrometer comprises separate trigger and high-precision tracking chambers measuring the deflection of muons in a magnetic field generated by the superconducting air-core toroidal magnets. The field integral of the toroids ranges between 2.0 and 6.0 T m across most of the detector. Three sets of precision chambers cover the region $|\eta| < 2.7$ with multiple layers of monitored drift tubes, complemented by cathode-strip chambers in the forward region, where the background is highest. The muon trigger system covers the range $|\eta| < 2.4$ with resistive-plate chambers in the barrel and thin-gap chambers in the endcap regions.

Interesting events are selected by the first-level trigger system implemented in custom hardware, followed by selections made by algorithms implemented in software in the high-level trigger [34]. The first-level trigger accepts events from the 40 MHz bunch crossings at a rate below 100 kHz, which the high-level trigger reduces in order to record events to disk at about 1 kHz.

An extensive software suite [35] is used in data simulation, in the reconstruction and analysis of real and simulated data, in detector operations, and in the trigger and data acquisition systems of the experiment.

3 Analysis strategy

A *CP*-sensitive observable φ^*_{CP} is built with different methods depending on the τ-lepton decay modes. In general, φ^*_{CP} is the signed acoplanarity angle between the τ-lepton decay planes. Each τ decay plane is constructed from the spatial momentum vector of a charged decay particle and either its impact parameter (impact parameter method) or the spatial momentum vectors of other visible τ-lepton decay particles (ρ-decay plane and a_1 methods). All vectors are boosted to the zero-momentum frame (ZMF) of the visible τ-lepton-pair decay particles. Figure 1a–c illustrate the methods used to construct the φ^*_{CP} observable in $H \to \tau^+\tau^- \to \pi^+\pi^- + 2\nu$, $H \to \tau^+\tau^- \to \pi^+\pi^0\nu\pi^-\pi^0\nu$ and $H \to \tau^+\tau^- \to \pi^+\pi^0\nu\pi^-\nu$ decays, respectively. The visible τ-lepton-pair ZMF (indicated by *) is used to approximate the Higgs boson rest frame, which is not accessible due to the presence of undetected neutrinos in the τ-lepton decays.

Figure 2 shows the normalised distribution of φ^*_{CP} for simulated $H \to \tau^+\tau^- \to \pi^+\pi^- + 2\nu$ events at the generator level. The distribution peaks at $\varphi^*_{CP} = 180°$ for a *CP*-even (e.g. SM) Higgs boson, whereas for the case of a pure *CP*-odd Higgs boson, the distribution peaks at $\varphi^*_{CP} = 0°$ and 360°. The phase difference between the φ^*_{CP} distributions for two different mixing scenarios is twice their ϕ_τ difference.

[2] ATLAS uses a right-handed coordinate system with its origin at the nominal interaction point in the centre of the detector and the z-axis along the beam pipe. The x-axis points from the interaction point to the centre of the LHC ring, and the y-axis points upwards. Cylindrical coordinates (r, ϕ) are used in the transverse plane, ϕ being the azimuthal angle around the z-axis. The pseudorapidity is defined in terms of the polar angle θ as $\eta = -\ln\tan(\theta/2)$. Angular distance is measured in units of $\Delta R \equiv \sqrt{(\Delta\eta)^2 + (\Delta\phi)^2}$.

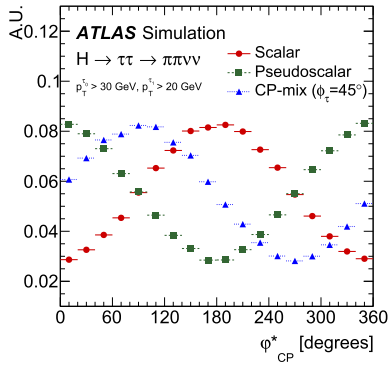

Fig. 2 Normalised φ^*_{CP} distributions in simulated $H \to \tau^+\tau^- \to \pi^+\pi^- + 2\nu$ events at the generator level for different *CP* hypotheses. The predictions for a pure *CP*-even SM Higgs boson (scalar, red circle), a pure *CP*-odd hypothesis (pseudoscalar, green square), and *CP*-mix hypothesis ($\phi_\tau = 45°$, blue triangle) are shown. The transverse momentum of the simulated τ leptons is required to be larger than 30 GeV (20 GeV) for the leading (sub-leading) τ lepton during the event generation

The τ-lepton-pair decay combinations used in the analysis and the respective methods for constructing the φ^*_{CP} observable are summarised in Table 2. The corresponding fraction of events relative to the total from all possible di-τ decay combinations is calculated from the single-τ-lepton decay mode branching fractions in Table 1. Other decay combinations are not considered in this analysis because their respective φ^*_{CP} observables perform relatively poorly in discriminating between different *CP* scenarios.

3.1 Impact parameter (IP) method

The IP method is applied to τ-lepton decays with only one charged particle in the final state, specifically the direct hadronic decay $\tau^\pm \to \pi^\pm\nu$ or leptonic decays $\tau^\pm \to \ell^\pm\nu\nu$. This refers to the 1p0n–1p0n and ℓ–1p0n decay mode combinations. In this case, the τ-lepton decay plane is formed from the spatial momentum vector $\mathbf{q}^\pm$ of the charged particle ($\pi^\pm$, $\ell^\pm$) and the three-dimensional (3D) impact parameter vector $\mathbf{n}^\pm$ of the charged particle, defined as the directional distance of closest approach of the charged particle's track to the reconstructed primary vertex (PV) of the event. The four-vectors of the track momentum $q^\pm_\mu$ and the impact parameter $n^\pm_\mu = (0, \mathbf{n}^\pm)$, initially defined and measured in the laboratory frame, are boosted to the rest frame of the two charged decay particles (the visible di-τ ZMF, denoted by *). The boosted and normalised impact parameter vector $\hat{\mathbf{n}}^{*\pm}$ is then decomposed into components which are parallel and transverse ($\hat{\mathbf{n}}^{*\pm}_\perp$) to the direction of the associated normalised spatial momentum vector $\hat{\mathbf{q}}^{*\pm}$. Using these vectors, an angle φ^* and a *CP*-odd triple correlation $\mathcal{O}^*_{CP}$ are defined as

$$\varphi^* = \arccos(\hat{\mathbf{n}}^{*+}_\perp \cdot \hat{\mathbf{n}}^{*-}_\perp) \quad \text{and} \quad \mathcal{O}^*_{CP} = \hat{\mathbf{q}}^{*-} \cdot (\hat{\mathbf{n}}^{*+}_\perp \times \hat{\mathbf{n}}^{*-}_\perp),$$

and both are incorporated in a single observable φ^*_{CP} ($0 \le \varphi^*_{CP} \le 360°$) defined by

$$\varphi^*_{CP} = \begin{cases} \varphi^* & \text{if } \mathcal{O}^*_{CP} \ge 0 \\ 360° - \varphi^* & \text{if } \mathcal{O}^*_{CP} < 0. \end{cases} \quad (1)$$

In the case of leptonic decay, due to a different sign in the spectral function for the leptonic τ decays [20,29], an additional shift by 180° is applied to synchronise the phase in φ^*_{CP} with the other decays.

3.2 ρ-decay plane (ρ) method

The ρ method is applied to construct φ^*_{CP} in events with 1p1n–1p1n or 1p1n–1pXn decay mode combinations. In the case of consecutive decays $\tau^\pm \to \rho^\pm\nu$, $\rho^\pm \to \pi^\pm\pi^0$, the τ-lepton decay plane can be formed from the spatial momentum vectors of the charged pion ($\mathbf{q}^\pm$) and neutral pion ($\mathbf{q}^{0\pm}$). The four-momentum vectors of the $\pi^\pm$ and π^0 are boosted to the rest frame of the ρ-meson pair (the visible τ-lepton-pair ZMF). The angle φ^* and triple correlation $\mathcal{O}^*_{CP}$ are then defined in the same way as in the IP method using the unit spatial vectors, but replacing the impact parameter component with the neutral-pion vector,

$$\varphi^* = \arccos(\hat{\mathbf{q}}^{*0+}_\perp \cdot \hat{\mathbf{q}}^{*0-}_\perp) \quad \text{and} \quad \mathcal{O}^*_{CP} = \hat{\mathbf{q}}^{*-} \cdot (\hat{\mathbf{q}}^{*0+}_\perp \times \hat{\mathbf{q}}^{*0-}_\perp),$$

where $\hat{\mathbf{q}}^{*0+}_\perp$ and $\hat{\mathbf{q}}^{*0-}_\perp$ are the normalised vectors transverse to the direction of the associated charged pion for each neutral pion. A signed observable $\varphi^{*\prime}$ is defined similarly to Eq. (1),

$$\varphi^{*\prime} = \begin{cases} \varphi^* & \text{if } \mathcal{O}^*_{CP} \ge 0 \\ 360° - \varphi^* & \text{if } \mathcal{O}^*_{CP} < 0. \end{cases}$$

An additional requirement that depends on the sign of the product of τ-lepton spin-analysing functions $y^\rho_\pm = (E_{\pi^\pm} - E_{\pi^0})/(E_{\pi^\pm} + E_{\pi^0})$, where $E_{\pi^{\pm,0}}$ is the pion energy in the laboratory frame, is needed to define the observable φ^*_{CP} sensitive to the *CP*-mixing angle as

$$\varphi^*_{CP} = \begin{cases} \varphi^{*\prime} & \text{if } y^\rho_+ y^\rho_- \ge 0 \\ \varphi^{*\prime} + 180° & \text{if } y^\rho_+ y^\rho_- < 0. \end{cases} \quad (2)$$

In the case of 1pXn decays (e.g. $\tau^\pm \to a_1^\pm\nu \to \pi^\pm 2\pi^0\nu$), the sum of the four-momenta of all neutral pions is taken as the neutral component in the ρ method.

3.3 Combined IP and ρ (IP–ρ) method

For events with the combinations 1p0n–1p1n, 1p0n–1pXn, ℓ–1p1n, and ℓ–1pXn, the IP method and the ρ method are combined to compute the φ^*_{CP} angle. In the case of $H \to \tau\tau \to \pi^\mp\nu\rho^\pm\nu$, $\rho^\pm \to \pi^\pm\pi^0$ (1p0n–1p1n) events, φ^*_{CP} is defined in the visible τ-lepton-pair ZMF by using the $\pi\rho$ rest frame. One of the decay planes is defined using the IP

Table 2 Decay mode combinations of the τ-lepton pair and the corresponding methods to construct the φ^*_{CP} observable used in this analysis. The fraction of events for each decay mode combination relative to the total from all di-τ decay combinations (last column) is calculated using the τ-lepton decay mode branching fractions in Table 1

Decay channel	Decay mode combination	Method	Fraction in all τ-lepton-pair decays (%)
$\tau_{\text{lep}}\ \tau_{\text{had}}$	ℓ–1p0n	IP	8.1
	ℓ–1p1n	IP–ρ	18.3
	ℓ–1pXn	IP–ρ	7.6
	ℓ–3p0n	IP–a_1	6.9
$\tau_{\text{had}}\ \tau_{\text{had}}$	1p0n–1p0n	IP	1.3
	1p0n–1p1n	IP–ρ	6.0
	1p1n–1p1n	ρ	6.7
	1p0n–1pXn	IP–ρ	2.5
	1p1n–1pXn	ρ	5.6
	1p1n–3p0n	ρ–a_1	5.1

method and the other with the ρ method. The quantities φ^*, $\mathcal{O}^*_{CP}$ and $\varphi^{*\prime}$ are calculated in a way analogous to that in Sect. 3.2, but with the one-neutral-pion component replaced with the impact parameter vector defined in Sect. 3.1. The φ^*_{CP} observable is defined as

$$\varphi^*_{CP} = \begin{cases} \varphi^{*\prime} & \text{if } y^\rho \geq 0 \\ \varphi^{*\prime} + 180^\circ & \text{if } y^\rho < 0, \end{cases} \tag{3}$$

with a phase shift of 180° depending on the sign of y^ρ.

3.4 a_1-decay (a_1) method

The a_1 method is an extension of the ρ method discussed in Sect. 3.2, and is used for $\tau^\pm \to a_1^\pm \nu$, $a_1^\pm \to \pi^\pm\pi^+\pi^-$. The τ-lepton decay plane is defined by the charged pion ($\pi_1^\pm$) with the highest transverse momentum and the vector sum of the other two π momenta. The observable $y^\rho_\pm$ used in the ρ method is modified to take the effect of the π masses into account, and is defined by $y^{a_1}_\pm$ adopting the convention in Ref. [36] as

$$y^{a_1}_\pm = \frac{E_{2\pi} - E_{\pi_1^\pm}}{E_{2\pi} + E_{\pi_1^\pm}} - \frac{m^2_{3\pi} - m^2_{\pi_1^\pm} + m^2_{2\pi}}{2m^2_{3\pi}},$$

where $m_{3\pi}$ is the invariant mass of the three charged pions from the $a_1^\pm$ decay, and $m_{2\pi}$ ($E_{2\pi}$) refers to the invariant mass (energy) of the system of the two π in the τ decay that do not have the highest transverse momentum.

Similarly to Sect. 3.3, the a_1 method is combined with the IP method for the ℓ–3p0n events and with the ρ method for the 1p1n–3p0n events in the $\tau_{\text{lep}}\ \tau_{\text{had}}$ and $\tau_{\text{had}}\ \tau_{\text{had}}$ channels, respectively. In the ℓ–3p0n case, φ^*_{CP} is defined similarly to Eq. (3), but with y^ρ replaced by y^{a_1}. For 1p1n–3p0n, the φ^*_{CP} computation is analogous to Eq. (2), except that the product $y^\rho_\pm y^{a_1}_\mp$ is used to determine whether the 180° shift is applied.

4 Data and simulated event samples

This analysis uses 139 fb^{-1} of $\sqrt{s} = 13$ TeV pp collision data recorded by ATLAS with good operating conditions [37] in 2015–2018. The data were collected using single-lepton or di-hadronic τ triggers [38–41]. Events used in the $\tau_{\text{lep}}\ \tau_{\text{had}}$ channel were accepted by single-lepton triggers with p_{T} thresholds of 24 GeV (26 GeV) and 20 GeV (26 GeV) for electron and muon candidates, respectively, in the 2015 (2016–2018) dataset. Events used in the $\tau_{\text{had}}\ \tau_{\text{had}}$ analysis channel were accepted by di-hadronic τ-lepton triggers, with a p_{T} threshold of 35 GeV for the leading τ candidate and 25 GeV for the sub-leading τ candidate. Due to rising instantaneous luminosity, the di-hadronic τ triggers used in the 2016–2018 data-taking period required an additional first-level triggered jet with $p_{\text{T}} > 25$ GeV and $|\eta| < 3.2$.

The analysis considers the four main Higgs boson production processes at the LHC: gluon–gluon fusion (ggF), vector-boson fusion (VBF), associated production with a vector boson (VH), and associated production with top-quark pair ($t\bar{t}H$). The POWHEG NNLOPS program [42–46] was used to model ggF Higgs boson production with next-to-next-leading-order (NNLO) accuracy. The VBF and VH production processes were simulated with POWHEG at NLO accuracy in QCD. The production of $t\bar{t}H$ events was simulated using POWHEG BOX v2 [44–48] at NLO with the NNPDF 3.0nlo [49] PDF set. In all signal events, the decays of τ-leptons were modelled by PYTHIA 8 [50] with no spin correlations. The spin correlations are reintroduced with event-by-event weights modelling CP-mixing-dependent transverse spin correlations, using the `TauSpinner` package [51–53]. Background samples of V + jets and diboson events were generated by SHERPA 2.2.1 [54] (including τ-lepton decays), and $t\bar{t}$ and single-top samples were generated by POWHEG+PYTHIA 8, with PYTHIA also performing τ-lepton decays. The simulated event samples are shared with the

cross-section measurement in the $H \to \tau\tau$ decay channel [55].

All samples of simulated events were passed through a full simulation of the ATLAS detector response [56] using GEANT4 [57]. The effects of multiple interactions in the same or neighbouring bunch crossings (pile-up) were modelled by overlaying each hard-scatter event with minimum-bias events, simulated using the soft QCD processes of PYTHIA 8. The simulated events were then weighted such that the distribution of the average number of interactions per bunch crossing matches the one observed in data.

5 Event selection and background estimation

The analysis of *CP*-mixing in the $H \to \tau\tau$ channel requires the selection of signal events characterised by the presence of isolated leptons, visible decay products in hadronic τ decays, jets and missing transverse momentum. Events with an isolated lepton (electron or muon) and a hadronic τ decay are used for the $\tau_{\text{lep}}\,\tau_{\text{had}}$ analysis channel, whereas events with two hadronic τ decays are used for the $\tau_{\text{had}}\,\tau_{\text{had}}$ channel. Additional jets, the invariant mass and the transverse momenta of the τ lepton pairs are used for event categorisation (Sect. 5.2). Various kinematic and identification requirements are used to suppress the background.

5.1 Objects and decay mode reconstruction

The analysis shares the same object reconstruction and identification algorithms as the $H \to \tau\tau$ cross-section measurement [55]. Here the most important features specific to this *CP* measurement are recalled:

- Tracks measured in the ID are used to reconstruct interaction vertices [58], of which the one with the highest sum of squared transverse momenta $\sum p_{\text{T}}^2$ of the associated tracks is selected as the primary vertex of the hard interaction.
- Electrons are reconstructed from topological clusters of energy deposits in the electromagnetic calorimeter which are matched to a track reconstructed in the ID [59] and are required to satisfy 'loose' isolation and 'medium' identification criteria.
- Muons are reconstructed from signals in the muon spectrometer matched with tracks inside the ID. They are required to satisfy 'loose' identification and 'tight' isolation criteria based on track information [60].
- Jets are reconstructed using a particle-flow algorithm [61]. It applies an anti-k_t algorithm [62,63] with distance parameter $R = 0.4$ to noise-suppressed positive-energy topological clusters in the calorimeter after subtracting energy deposits associated with primary-vertex-matched tracks, and including the track momenta instead in the clustering, thereby improving the jet energy measurement. Cleaning criteria are used to identify jets arising from non-collision backgrounds or noise in the calorimeters [64]. A dedicated jet-vertex-tagger algorithm [65] is used to remove jets that are identified as not being associated with the primary vertex of the hard interaction. Similarly, a dedicated algorithm is used to suppress pile-up jets in the forward region [66].
- Hadronic τ-lepton decays are reconstructed from the visible decay products (neutral pions or charged pions/kaons). The reconstruction is seeded by jets reconstructed with an anti-k_t algorithm using calibrated topological clusters [67] as inputs and a distance parameter of $R = 0.4$ [68]. Reconstructed nearby tracks are matched to a hadronic τ candidate ($\tau_{\text{had-vis}}$) if they exceed the value required for a multivariate discriminant determining the likelihood that the tracks are produced from the $\tau_{\text{had-vis}}$ decay. A recurrent neural network identification algorithm [69] is trained to separate the $\tau_{\text{had-vis}}$ candidates from jets initiated by quarks or gluons, and boosted decision tree (BDT) discriminants are used to help reject misidentified hadronic τ decays due to electrons. In both cases, the $\tau_{\text{had-vis}}$ is required to satisfy 'medium' criteria. Reconstructed $\tau_{\text{had-vis}}$ objects are required to have one or three associated tracks, and have $p_{\text{T}} > 20$ GeV and $|\eta| < 2.47$, excluding the transition region between the barrel and endcap electromagnetic calorimeters ($1.37 < |\eta| < 1.52$).
- The missing transverse momentum (with magnitude $E_{\text{T}}^{\text{miss}}$) is reconstructed as the negative vector sum of the transverse momenta of leptons, $\tau_{\text{had-vis}}$ objects, jets, and a 'soft-term'. The 'soft-term' is calculated as the vector sum of the p_{T} of tracks matched to the primary vertex but not associated with reconstructed leptons, $\tau_{\text{had-vis}}$ objects, or jets [70].
- The invariant mass of the τ-lepton-pair system, $m_{\tau\tau}^{\text{MMC}}$, is estimated with an advanced likelihood-based algorithm named the Missing Mass Calculator (MMC) [55,71].

The transverse (longitudinal) impact parameter d_0 (z_0) of a charged-particle track is defined as the distance in the transverse plane (z direction) from the primary vertex to the track's point of closest approach in the transverse plane. The impact parameters are used in the calculation of the φ_{CP}^* observable in the cases involving single-pion or leptonic decays (Sect. 3.1), as well as in one of the variables defining the signal regions (Sect. 5.2).

An important addition in the *CP* analysis is that it requires the τ-lepton reconstruction algorithms to categorise the hadronic τ-lepton decays by using the number of reconstructed tracks and the capability to distinguish between single-π^0 and multi-π^0 clusters. This allows the

τ_{had} candidates to be classified as being from the 1p0n, 1p1n, 1pXn or 3p0n decay modes. For this measurement it is crucial to identify each decay mode with good efficiency and purity, and to measure the momenta of the charged and neutral pions. This is achieved through the 'τ_{had} Particle Flow' reconstruction algorithm [72], in which the four-momenta of the charged and neutral pions from the τ decay are determined by combining measurements from the tracking detector and the calorimeter. The decay mode classification is performed by counting the number of charged and neutral pions, exploiting the kinematic properties of the τ-lepton decay products and the number of reconstructed photons by using BDTs. Three BDTs are built respectively for the 1p0n vs 1p1n, 1p1n vs 1pXn and 3p0n vs 3pXn decay modes to improve the determination of the number of neutral pions in each case. The efficiency (purity) of the classification is about 80% (70–80%) for the dominant decay modes 1p0n and 1p1n; for the 3p0n decay mode the efficiency is over 90%, with 90% purity.

5.2 Event selection

Events are selected by requiring at least one hadronic τ-lepton decay in the signature. For events in the $\tau_{\text{lep}}\,\tau_{\text{had}}$ channel, a $\tau_{\text{had-vis}}$ with $p_{\text{T}} > 30$ GeV and an electron or muon with $p_{\text{T}} > 21.0{-}27.3$ GeV are required, with the latter p_{T} cut depending on the data-taking period. In the $\tau_{\text{had}}\,\tau_{\text{had}}$ channel, two $\tau_{\text{had-vis}}$ objects are required with p_{T} above 40 and 30 GeV. The p_{T} requirements are chosen to be above the p_{T} thresholds of the respective single-lepton and hadronic τ triggers to ensure trigger operation at the plateau efficiency. The $\tau_{\text{had-vis}}$ and the lepton are required to match geometrically with their trigger counterparts in the $\tau_{\text{had}}\,\tau_{\text{had}}$ and $\tau_{\text{lep}}\,\tau_{\text{had}}$ channels, respectively. In both channels the two τ-lepton candidates are required to have opposite electric charges. The angular distances between the τ-lepton candidates are required to be $\Delta R_{\tau\tau} < 2.5$ and $|\Delta\eta_{\tau\tau}| < 1.5$ ($0.6 < \Delta R_{\tau\tau} < 2.5$ and $|\Delta\eta_{\tau\tau}| < 1.5$) to reject non-resonant events in the $\tau_{\text{lep}}\,\tau_{\text{had}}$ ($\tau_{\text{had}}\,\tau_{\text{had}}$) channel. All events require at least one jet with $p_{\text{T}} > 40$ GeV. Due to triggering conditions, this selection is tightened to $p_{\text{T}} > 70$ GeV and $|\eta| < 3.2$ in the $\tau_{\text{had}}\,\tau_{\text{had}}$ channel. The $E_{\text{T}}^{\text{miss}}$ is required to be greater than 20 GeV, and requirements on the fraction of the τ-lepton momentum carried by its visible decay products are applied to further improve the invariant mass estimation. In the $\tau_{\text{lep}}\,\tau_{\text{had}}$ channel, the transverse mass m_{T} of the lepton-plus-$E_{\text{T}}^{\text{miss}}$ system is required to be less than 70 GeV in order to efficiently reject W+jets processes. These preselection criteria are the same as in the $H \to \tau\tau$ cross-section measurement [55].

Events are further categorised to target the vector-boson fusion (VBF category) and gluon–gluon fusion (Boost category) Higgs boson production modes. The VBF category contains events with a second high-p_{T} jet with $p_{\text{T}}^{j_2} > 30$ GeV. The two leading jets are required to satisfy the following kinematics: $|\Delta\eta_{jj}| > 3.0$, $\eta_{j_1} \cdot \eta_{j_2} < 0$, and $m_{jj} > 400$ GeV, with the pseudorapidity values of τ_{lep} or τ_{had} lying between those of the two leading jets (yielding 'central τ-leptons'). This kinematic selection is enhanced by splitting the VBF category into two regions, VBF_1 and VBF_0, based on the output of a BDT-based VBF tagger [55], with the VBF_1 region having an enhanced fraction of VBF Higgs boson production events. The Boost category targets events where the Higgs boson recoils against jets. The p_{T} of the Higgs boson ($p_{\text{T}}^{\tau\tau}$) is computed as the magnitude of the vector sum of the transverse momenta of the τ-leptons' visible decay products and the missing transverse momentum. Events with $p_{\text{T}}^{\tau\tau} > 100$ GeV that do not pass the VBF selection form the Boost category. These events are further separated into those with $\Delta R_{\tau\tau} < 1.5$ and $p_{\text{T}}^{\tau\tau} > 140$ GeV (Boost_1) and those not passing these selections (Boost_0). The event categorisation is applied to both the $\tau_{\text{lep}}\,\tau_{\text{had}}$ and $\tau_{\text{had}}\,\tau_{\text{had}}$ channels, as summarised in Table 3.

For each category, a Higgs-enriched signal region is defined with $110 < m_{\tau\tau}^{\text{MMC}} < 150$ GeV, and a $Z \to \tau\tau$ control region (CR) is defined with $60 < m_{\tau\tau}^{\text{MMC}} < 110$ GeV, with the other selection criteria for each category remaining the same. Two additional control regions are defined using events with a $\tau^{\pm} \to \rho^{\pm}\nu \to \pi^{\pm}\pi^{0}\nu$ decay in the $60 < m_{\tau\tau}^{\text{MMC}} < 110$ GeV range: one region with ℓ–1p1n events for the $\tau_{\text{lep}}\,\tau_{\text{had}}$ channel, and the other with 1p1n–1p1n events for the $\tau_{\text{had}}\,\tau_{\text{had}}$ channel. The events in these regions are defined so as to be statistically independent of the four $Z \to \tau\tau$ control regions in Table 3. The use of the control regions is described in Sect. 7.

Depending on the decay mode combination, different additional selection criteria are applied to enhance the sensitivity of the φ_{CP}^{*} construction method. The φ_{CP}^{*} from the IP method is less effective in discriminating between different ϕ_{τ} values when the impact parameter vector has a magnitude smaller than, or similar to, its resolution. The sensitivity of this method can be enhanced by using events with high significance of the track impact parameter in the transverse plane, d_0^{sig}, defined as the transverse impact parameter d_0 divided by its resolution $\sigma(d_0)$. Events are therefore separated into two groups based on the value of $|d_0^{\text{sig}}|$ of the lepton in τ_{lep} or the pion in τ_{had}. In the ρ method, events with larger absolute values of the product $|y_{+}^{\rho} y_{-}^{\rho}|$ are more sensitive to ϕ_{τ}. This quantity is also used to separate the events into two groups. In the case of the combined IP–ρ method, the sensitivity of φ_{CP}^{*} is enhanced by separating the events based on the values $|d_0^{\text{sig}}|$ and $|y^{\rho}|$. For the IP–a_1 and ρ–a_1 methods the separation is based on $|y_{\pm}^{a_1}|$. Details of the additional selection criteria are summarised in Tables 4 and 5.

Table 3 Summary of selection criteria for the VBF and Boost categories in this analysis. The criteria are common to the $\tau_{\text{lep}}\,\tau_{\text{had}}$ and $\tau_{\text{had}}\,\tau_{\text{had}}$ decay channels

VBF		Boost	
$p_{\text{T}}^{j_2} > 30$ GeV $m_{jj} > 400$ GeV $\lvert\Delta\eta_{jj}\rvert > 3.0$ $\eta_{j_1} \cdot \eta_{j_2} < 0$ Central τ-leptons		Not VBF $p_{\text{T}}^{\tau\tau} > 100$ GeV	
Signal region ($110 < m_{\tau\tau}^{\text{MMC}} < 150$ GeV)			
VBF_1	VBF_0	Boost_1	Boost_0
BDT(VBF) > 0	BDT(VBF) < 0	$\Delta R_{\tau\tau} < 1.5$ and $p_{\text{T}}^{\tau\tau} > 140$ GeV	$\Delta R_{\tau\tau} > 1.5$ or $p_{\text{T}}^{\tau\tau} < 140$ GeV
$Z \to \tau\tau$ control region ($60 < m_{\tau\tau}^{\text{MMC}} < 110$ GeV)			
VBF_1 Z CR	VBF_0 Z CR	Boost_1 Z CR	Boost_0 Z CR

Among the τ-lepton pair decays used in this analysis, the most sensitive ('dominant') decay mode combinations are 1p0n–1p1n, 1p1n–1p1n, and 1p0n–1p0n in the $\tau_{\text{had}}\,\tau_{\text{had}}$ decay channel, and ℓ–1p1n and ℓ–1p0n in the $\tau_{\text{lep}}\,\tau_{\text{had}}$ decay channel, while the other combinations involving 1pXn and 3p0n are subdominant due to their weaker spin analysing power and smaller decay fractions. The events are therefore divided into three groups, the 'High', 'Medium' and 'Low' signal regions, which characterise the different levels of sensitivity. Events satisfying the additional selection criteria for the dominant and subdominant decay mode combinations define the High and Medium signal regions, respectively, while the rest are grouped into the Low signal region. This allows the φ_{CP}^{*} distributions from the decay mode combinations with similar sensitivity to *CP*-mixing to be merged to increase the statistical precision of the distribution templates within each signal region, allowing the use of finer binning in the φ_{CP}^{*} distributions for the regions with better sensitivity. The splitting of the signal regions summarised in Tables 4 and 5 is applied in each of the VBF and Boost categories (VBF_1, VBF_0, Boost_1 and Boost_0).

In this configuration, there are 12 signal regions in each of the $\tau_{\text{lep}}\,\tau_{\text{had}}$ and $\tau_{\text{had}}\,\tau_{\text{had}}$ decay channels, leading to 24 signal regions in total. Each signal or control region is orthogonal to the others.

5.3 Background estimation

Expected SM processes other than the $H \to \tau\tau$ signal are evaluated using a mixture of simulation and data-driven techniques. Processes with true τ-leptons and prompt light leptons are estimated through simulation. Among those the $Z(\to \tau\tau)$ + jets process is the dominant one, and dedicated control regions with $60 < m_{\tau\tau}^{\text{MMC}} < 110$ GeV (Sect. 5.2) are used to extract its normalisation (Sect. 7).

The second most significant background contribution arises from jets misidentified as hadronically decaying τ-leptons (τ_{had}), referred to as 'misidentified-τ background'. It is determined by a data-driven approach using fake factors, as described in detail in Ref. [55]. The misidentified-τ background consists mostly of W+jets, QCD multijet, and top-quark events in the $\tau_{\text{lep}}\,\tau_{\text{had}}$ channel, while in the $\tau_{\text{had}}\,\tau_{\text{had}}$ channel it originates mainly from multijet events. The fake factors are calculated as the ratio of the number of events passing the τ identification requirements to the number failing them in dedicated QCD and W+jets -enriched regions, defined by inverting the lepton isolation or m_{T} requirement, respectively. The fake factors are estimated in each hadronic τ decay mode considered in the analysis, separately for VBF and Boost region events. To estimate both the shape and the normalisation of the misidentified-τ background, distributions in the regions failing the τ identification are multiplied by the fake factors to correct for the different efficiencies to pass or fail the τ identification selection. In the 'failed τ identification' regions, events not corresponding to misidentified-τ background from jets are subtracted using simulated event samples. For the $\tau_{\text{had}}\,\tau_{\text{had}}$ final state the fake-factor method is modified slightly: the τ_{had} objects are matched to their trigger counterparts and the estimate covers processes with one or two jets misidentified as τ_{had}. The misidentified-τ background contribution is estimated for each di-τ decay combination considered (Sect. 3) in the preselection region for the $\tau_{\text{had}}\,\tau_{\text{had}}$ events.

Smaller background contributions are due to diboson, $Z(\to \ell\ell)$ + jets and $H \to WW^{*}$ processes in both decay channels, while W+jets and top production also make small

Table 4 Summary of additional selection criteria for the signal regions in the $\tau_{\text{lep}}\,\tau_{\text{had}}$ channel

Channel	Signal region	Decay mode combination	Selection criteria
$\tau_{\text{lep}}\,\tau_{\text{had}}$	High	ℓ–1p0n	$\lvert d_0^{\text{sig}}\,(e)\rvert > 2.5$ or $\lvert d_0^{\text{sig}}\,(\mu)\rvert > 2.0$ $\lvert d_0^{\text{sig}}\,(\tau_{\text{1p0n}})\rvert > 1.5$
		ℓ–1p1n	$\lvert d_0^{\text{sig}}\,(e)\rvert > 2.5$ or $\lvert d_0^{\text{sig}}\,(\mu)\rvert > 2.0$ $\lvert y^{\rho}(\tau_{\text{1p1n}})\rvert > 0.1$
	Medium	ℓ–1pXn	$\lvert d_0^{\text{sig}}\,(e)\rvert > 2.5$ or $\lvert d_0^{\text{sig}}\,(\mu)\rvert > 2.0$ $\lvert y^{\rho}(\tau_{\text{1pXn}})\rvert > 0.1$
		ℓ–3p0n	$\lvert d_0^{\text{sig}}\,(e)\rvert > 2.5$ or $\lvert d_0^{\text{sig}}\,(\mu)\rvert > 2.0$ $\lvert y^{a_1}(\tau_{\text{3p0n}})\rvert > 0.6$
	Low	All above	Not satisfying selection criteria

Table 5 Summary of additional selection criteria for the signal regions in the $\tau_{\text{had}}\,\tau_{\text{had}}$ channel

Channel	Signal region	Decay mode combination	Selection criteria
$\tau_{\text{had}}\,\tau_{\text{had}}$	High	1p0n–1p0n	$\lvert d_0^{\text{sig}}\,(\tau_1)\rvert > 1.5$ $\lvert d_0^{\text{sig}}\,(\tau_2)\rvert > 1.5$
		1p0n–1p1n	$\lvert d_0^{\text{sig}}\,(\tau_{\text{1p0n}})\rvert > 1.5$ $\lvert y^{\rho}(\tau_{\text{1p1n}})\rvert > 0.1$
		1p1n–1p1n	$\lvert y^{\rho}(\tau_1)y^{\rho}(\tau_2)\rvert > 0.2$
	Medium	1p0n–1pXn	$\lvert d_0^{\text{sig}}\,(\tau_{\text{1p0n}})\rvert > 1.5$ $\lvert y^{\rho}(\tau_{\text{1pXn}})\rvert > 0.1$
		1p1n–1pXn	$\lvert y^{\rho}(\tau_{\text{1p1n}})y^{\rho}(\tau_{\text{1pXn}})\rvert > 0.2$
		1p1n–3p0n	$\lvert y^{\rho}(\tau_{\text{1p1n}})\rvert > 0.1$ $\lvert y^{a_1}(\tau_{\text{3p0n}})\rvert > 0.6$
	Low	All above	Not satisfying selection criteria

contributions in the $\tau_{\text{had}}\,\tau_{\text{had}}$ channel. These are estimated from simulation and are normalised to their theoretical expectations.

6 Systematic uncertainties

Systematic uncertainties generally affect the yield in the signal and control regions as well as the shape of the φ^*_{CP} distribution, on which the fit is performed. They are grouped into three types: the experimental uncertainties, the theoretical uncertainties, and the τ-lepton decay reconstruction uncertainties.

The experimental uncertainties include those from the trigger, reconstruction, identification and isolation requirements of the final-state particle candidates (electrons, muons, τ-leptons, jets, $E_{\text{T}}^{\text{miss}}$, b-tagging), as well as uncertainties from misidentified-τ background estimation and the luminosity measurement [73,74].

The uncertainties on the jet energy resolution and scale [75] affect the acceptance of the signal and background contributions through their impact on $E_{\text{T}}^{\text{miss}}$, and thus $m_{\tau\tau}^{\text{MMC}}$ [76]. They also directly affect the jet selection for the event categorisation in the VBF and Boost regions [76]. The jet energy scale uncertainty for central jets ($|\eta| < 1.2$) varies from 1% for a wide range of jet p_{T} (250 GeV $< p_{\text{T}} <$ 2000 GeV) to 5% for very low p_{T} jets ($p_{\text{T}} < 20$ GeV), and 3.5% for very high p_{T} jets ($p_{\text{T}} > 2.5$ TeV), and forward jets exhibit uncertainties of similar size. The relative jet energy resolution ranges from (24 ± 1.5)% to (6 ± 0.5)% for jets with p_{T} of 20 GeV to 300 GeV, respectively [75]. Other jet-related uncertainties have smaller impacts.

Uncertainties from the misidentified-τ background estimation arise from sample statistics of the events used for estimating the fake factors, subtraction of residual contributions from processes without misidentified-τ, and uncertainties in the flavour composition taken from comparisons between the predicted and observed backgrounds in a dedicated validation region. The uncertainties are assigned per τ-lepton-pair decay combination in the $\tau_{\text{lep}}\,\tau_{\text{had}}$ and $\tau_{\text{had}}\,\tau_{\text{had}}$ channels. The total expected uncertainties in the yield of the misidentified-τ events in the signal regions are typically 20% (20–40%) in the Boost (VBF) region in the $\tau_{\text{lep}}\,\tau_{\text{had}}$ channel, and 15–30% in the $\tau_{\text{had}}\,\tau_{\text{had}}$ channel.

Theoretical uncertainties are applied to Z+jets background and signal processes. For the Z + jets background, uncertainties are considered for the renormalisation and factorisation scales, the resummation scale, the jet-to-parton matching scheme, the choice of value for the strong coupling constant α_s, and the choice of PDF. Only distribution shapes and migrations between analysis regions are considered for these uncertainties since the absolute normalisation of $Z \to \tau\tau$ is determined at the fit level. For the signal, uncertainties are considered for the QCD scale because of missing higher orders in the matrix element calculation, for the parton shower and hadronisation model, and for renormalisation and factorisation scales and the PDF. These are applied to the production cross-sections for the ggF, VBF and VH processes, and do not have large impacts on the measurement as they only affect the signal normalisation, which is also determined in the fit, and not the shape of the φ^*_{CP} distribution.

The τ-lepton decay reconstruction uncertainties primarily affect the shape of the φ^*_{CP} distributions. These concern the classification of the hadronic τ-lepton decay modes as well as measurement uncertainties of the track impact parameters, pion track momentum, and neutral pion momentum. The uncertainties in the classification of the hadronic τ-lepton decay modes are derived from a τ-lepton decay mode classification efficiency and correction factor measurement, using a tag-and-probe analysis in the μ–τ_{had} final state performed on part of the Run 2 dataset. These uncertainties include those in the decay mode reconstruction efficiencies and in the event migration between decay modes. The size of the uncertainties ranges from 6 to 20% depending on the decay modes and their cross migrations. The uncertainties affecting the impact parameters and track measurements include those in alignment effects and in impact parameter resolution, and they account for differences between data and simulation.

The uncertainties in the π^0 angular resolution and energy scale are estimated in situ in the analysis. The π^0 energy and momentum direction are initially varied in accordance with the energy response of the calorimeter to charged pions [77] and the measured π^0 angular resolution [72], respectively. These variations in the π^0 energy scale and angular resolution are found to affect the shape of the distribution of the reconstructed invariant mass of the $\pi^\pm\pi^0$ system, $m(\pi^\pm, \pi^0)$, in $\tau^\pm \to \rho^\pm\nu \to \pi^\pm\pi^0\nu$ decays. Dedicated $Z \to \tau\tau$ control regions with exclusive 1p1n decays, namely the ℓ–1p1n and 1p1n–1p1n events, are defined in the $\tau_{\text{lep}}\,\tau_{\text{had}}$ and $\tau_{\text{had}}\,\tau_{\text{had}}$ decay channels, respectively, as described in Sect. 5.2. The $m(\pi^\pm, \pi^0)$ distribution is used as the observable in these control regions in the combined fit, so that the final size of the π^0 angular resolution and energy scale uncertainties in the ϕ_τ measurement are determined from data. Figure 3 shows the post-fit distributions of $m(\pi^\pm, \pi^0)$ in the $Z \to \tau\tau$ control regions in the $\tau_{\text{lep}}\,\tau_{\text{had}}$ and $\tau_{\text{had}}\,\tau_{\text{had}}$ channels using ℓ–1p1n and 1p1n–1p1n events, respectively. For the 1p1n–1p1n events in the $\tau_{\text{had}}\,\tau_{\text{had}}$ channel, only the leading τ_{had} is selected for the $m(\pi^\pm, \pi^0)$ distribution. The $m(\pi^\pm, \pi^0)$ data distributions show good agreement with the prediction.

7 Statistical analysis

To measure the CP-mixing angle ϕ_τ, a simultaneous fit to the data is performed using a likelihood function that depends on the CP-mixing angle ϕ_τ as the parameter-of-interest, and the nuisance parameters that account for the systematic uncertainties and the floating normalisations for the Higgs boson signal and for the background. The likelihood function is constructed as a product of Poisson probability terms over the bins of the input distributions, and the parameter-of-interest is estimated by maximising the likelihood. The likelihood comprises 24 signal regions and 10 control regions. Constraints on the nuisance parameters are assigned with a Gaussian term, and bin-by-bin statistical fluctuations in the simulated background samples are included in the fit with a Poisson probability term.

In the fit the normalisation of the $Z \to \tau\tau$ events is left to float freely in the eight control regions (described in Sect. 5.2) to account for the $Z \to \tau\tau$ modelling in the different signal regions. Four normalisation factors (NF) are defined to control the $Z \to \tau\tau$ background events in the Boost_0, Boost_1, VBF_0, VBF_1 categories, respectively. Each factor is shared between the $\tau_{\text{lep}}\,\tau_{\text{had}}$ and $\tau_{\text{had}}\,\tau_{\text{had}}$ channels, and is also shared between a control region and the corresponding signal region in the same category. Other backgrounds are normalised to their expected number of events estimated from the MC simulation.

Two control regions using events with a $\tau^\pm \to \rho^\pm\nu \to \pi^\pm\pi^0\nu$ decay (ℓ–1p1n in $\tau_{\text{lep}}\,\tau_{\text{had}}$ and 1p1n–1p1n in $\tau_{\text{had}}\,\tau_{\text{had}}$) are defined from the $Z \to \tau\tau$ control region events (Sect. 5.2). The distribution of the $\pi^\pm\pi^0$ invariant mass, $m(\pi^\pm, \pi^0)$, is employed in these control regions to control the π^0-related uncertainties by using the data, as described in Sect. 6.

The Higgs boson signal strength $\mu_{\tau\tau}$ (defined as the ratio of the measured signal yield to the SM expectation) is also left unconstrained in the fit, such that the signal normalisation does not depend on the SM assumption and only the shape of the φ^*_{CP} distribution is exploited in the estimation of ϕ_τ. Model-dependence of the cross-section on CP-mixing scenarios is not exploited. The φ^*_{CP} distributions in the signal regions are binned to maximise the measurement sensitivity, taking into account the associated uncertainties. In general, finer binnings are used in the signal regions associated with higher sensitivity (High and Medium SRs), with coarser binning in the Low signal region. A smoothing procedure is applied in the signal regions to remove potentially

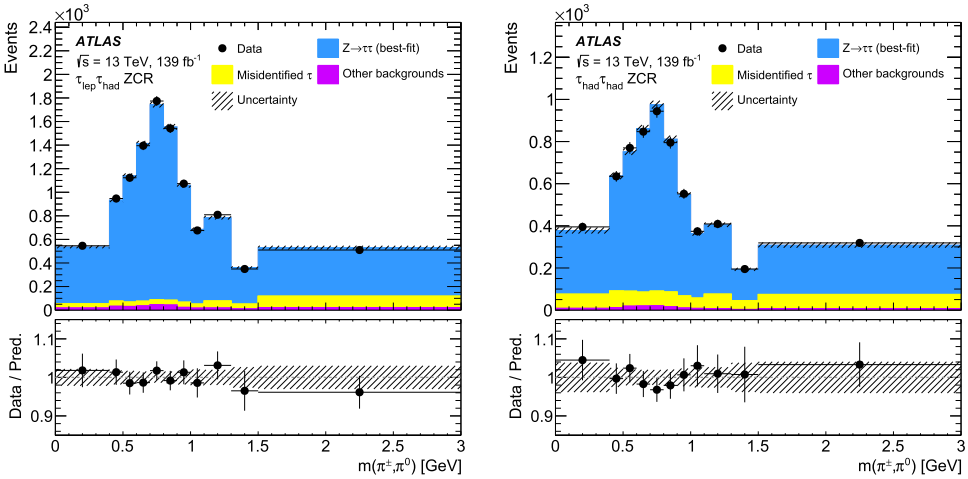

(a) $\tau_{\text{lep}}\tau_{\text{had}}$ ZCR with ℓ–1p1n events (b) $\tau_{\text{had}}\tau_{\text{had}}$ ZCR with 1p1n–1p1n events

Fig. 3 Post-fit distributions of the $\pi^{\pm}\pi^{0}$ invariant mass, $m(\pi^{\pm},\pi^{0})$, in the $Z \to \tau\tau$ control regions in the **a** τ_{lep} τ_{had} and **b** τ_{had} τ_{had} channels. The ℓ–1p1n (1p1n–1p1n) events are used in the τ_{lep} τ_{had} (τ_{had} τ_{had}) channel in this control region. For the τ_{had} τ_{had} channel only the $m(\pi^{\pm},\pi^{0})$ value of the leading τ_{had} is selected. 'Other backgrounds' include W, diboson, top, $Z \to \ell\ell$ and $H \to WW^{*}$. The hatched uncertainty band includes all sources of uncertainty after the fit to data

large local fluctuations in the systematic variations of the φ^{*}_{CP} distributions because of the limited size of the MC samples used to build the templates. The test statistic is based on a profile likelihood ratio and the asymptotic approximation [78] is used for statistical interpretations.

8 Results

Figure 4 shows the post-fit φ^{*}_{CP} distributions for the data as well as the prediction in the High, Medium and Low signal regions in the τ_{lep} τ_{had} and τ_{had} τ_{had} channels, respectively. In each distribution, the φ^{*}_{CP} bins are counted incrementally through all VBF and Boost categories and cover the range [0, 360]° for each category. The observed and expected negative log-likelihood ($\Delta \ln L$) scans in ϕ_{τ} are shown in Fig. 5. The observed (expected) value of ϕ_{τ} is $9° \pm 16°$ ($0° \pm 28°$) at the 68% confidence level (CL), and $\pm 34°$ ($^{+75°}_{-70°}$) at the 2σ level. The data disfavours the pure CP-odd hypothesis at the 3.4σ level, while the expected exclusion level is 2.1σ. The fitted signal and background normalisations are shown in Table 6. The results are compatible with the SM expectation within the measured uncertainties.

The total uncertainty is dominated by the statistical uncertainties of the data sample. The dominant contributions to the systematic uncertainties are from jets, followed by limited sample size of the background simulations, uncertainties from the free-floating normalisation factors, and theory uncertainties. The uncertainties in the τ-lepton decay reconstruction have small impacts of less than 1° on ϕ_{τ}. The effects from the π^{0} uncertainties measured in situ are compared with those from a set of simulated event samples with systematically varied modelling of the hadronic response in the calorimeter, and the latter are found to have a similar impact on the ϕ_{τ} measurement. Effects from other sources are negligible. The impact of the uncertainties is summarised in Table 7.

The difference between the observed and expected sensitivities of the ϕ_{τ} measurement can be attributed to a statistical fluctuation in data. The uncertainties of the ϕ_{τ} measurement are highly dependent on the size of the modulation amplitude of the φ^{*}_{CP} distributions. In the measured data, there are more distortions of the φ^{*}_{CP} shape due to bins fluctuating from their expected values, resulting in overall larger modulation amplitudes than the predicted shape. A set of pseudo-experiments is performed (with the condition $\mu_{\tau\tau} = 1$) that shows that the probability of obtaining the observed distribution, given the expectation, is about 4%.

The present measurement is compatible with the recent measurement of the same mixing-angle parameter by the CMS Collaboration [24], for which an observed (expected) mixing-angle value of $-1° \pm 19°$ ($0° \pm 21°$) at the 68% CL was reported.

The expected sensitivities of the τ_{had} τ_{had} and τ_{lep} τ_{had} channels in excluding a pure CP-odd $H\tau\tau$ coupling are 1.7σ and 1.1σ, respectively. The 'High' signal regions contribute the most, with 1.4σ and 1.0σ in the τ_{had} τ_{had} and τ_{lep} τ_{had} channels, respectively. Other signal regions have expected sensitivities below 1σ.

A 2D scan of $\Delta \ln L$ as a function of the signal strength $\mu_{\tau\tau}$ versus ϕ_{τ} is shown in Fig. 6. The 1σ and 2σ 2D confidence levels correspond to $\Delta \ln L$ values of 1.15 and 3.09, respectively. No strong correlation between $\mu_{\tau\tau}$ and ϕ_{τ} is observed. The SM prediction of $\mu_{\tau\tau} = 1$ and $\phi_{\tau} = 0$ is compatible with the measurement within the 1σ confidence region.

Figure 7 shows the data distribution of φ^{*}_{CP} with all signal regions in both the τ_{lep} τ_{had} and τ_{had} τ_{had} channels combined, together with the best-fit $H \to \tau\tau$ signal, pure CP-even and

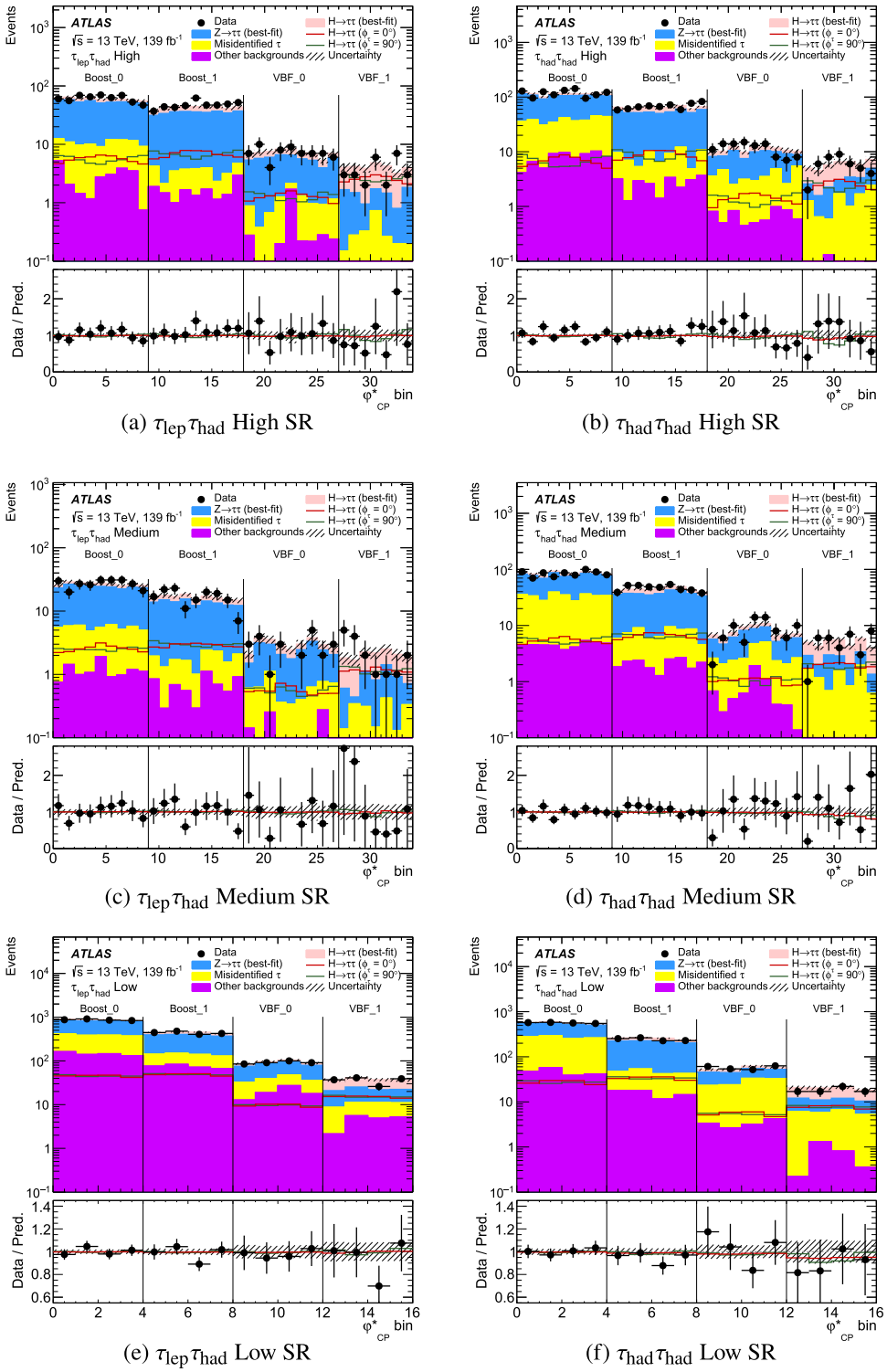

(a) $\tau_{\text{lep}}\tau_{\text{had}}$ High SR (b) $\tau_{\text{had}}\tau_{\text{had}}$ High SR

(c) $\tau_{\text{lep}}\tau_{\text{had}}$ Medium SR (d) $\tau_{\text{had}}\tau_{\text{had}}$ Medium SR

(e) $\tau_{\text{lep}}\tau_{\text{had}}$ Low SR (f) $\tau_{\text{had}}\tau_{\text{had}}$ Low SR

Fig. 4 Post-fit distributions of φ^*_{CP} in the signal regions (SRs), showing **a** τ_{lep} τ_{had} High SR, **b** τ_{had} τ_{had} High SR, **c** τ_{lep} τ_{had} Medium SR, **d** τ_{had} τ_{had} Medium SR, **e** τ_{lep} τ_{had} Low SR, and **f** τ_{had} τ_{had} Low SR. The φ^*_{CP} bins are counted incrementally through all VBF and Boost categories and cover the range [0, 360]° for each category. The best-fit $H \to \tau\tau$ signal is shown in solid pink, while the red and green lines indicate the predictions for the pure *CP*-even (scalar, SM) and pure *CP*-odd (pseudoscalar) hypotheses, respectively, scaled to the predicted signal yield. 'Other backgrounds' include W, diboson, top, $Z \to \ell\ell$ and $H \to WW^*$. The hatched uncertainty band includes all sources of uncertainty after the fit to data

pure *CP*-odd hypotheses. The events in each signal region are weighted with $\ln(1 + S/B)$, where S and B are the event yields for the signal and the total background, respectively. The background is subtracted from data in the figure. The distribution illustrates that the data disfavours the pure *CP*-odd scenario.

9 Conclusion

A measurement of the *CP* properties of the interaction between the Higgs boson and τ-leptons is presented. In the generalised Yukawa interaction, a single mixing parameter ϕ_τ parameterises *CP*-violating interactions between the Higgs boson and τ-leptons. The measurement is performed

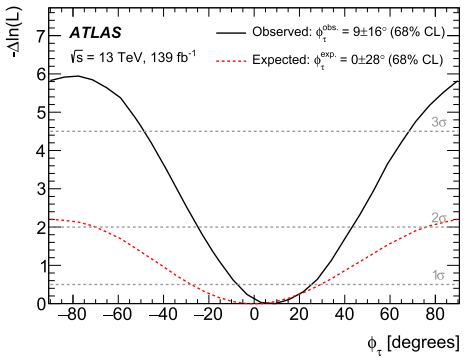

Fig. 5 One-dimensional likelihood scan of the *CP*-mixing angle ϕ_τ. The observed (expected) value of ϕ_τ is $9° \pm 16°$ ($0° \pm 28°$) at the 68% confidence level (CL), and $\pm 34°$ ($^{+75°}_{-70°}$) at the 2σ level. The *CP*-odd hypothesis is rejected at the 3.4σ (2.1σ expected) level

Table 6 Free-floating parameters in the measurement. Observed and expected values are shown for the *CP*-mixing angle (ϕ_τ), the signal strength ($\mu_{\tau\tau}$) and various background normalisations for $Z \to \tau\tau$ ($\mathrm{NF}_{Z\to\tau\tau}$) corresponding to different signal phase-space regions

Fitted parameters	Observed	Expected
ϕ_τ	$9° \pm 16°$	$0° \pm 28°$
$\mu_{\tau\tau}$	$1.02^{+0.20}_{-0.20}$	$1.00^{+0.21}_{-0.21}$
$\mathrm{NF}^{\mathrm{Boost_1}}_{Z\to\tau\tau}$	1.01 ± 0.05	1.00 ± 0.04
$\mathrm{NF}^{\mathrm{Boost_0}}_{Z\to\tau\tau}$	1.02 ± 0.05	1.00 ± 0.05
$\mathrm{NF}^{\mathrm{VBF_1}}_{Z\to\tau\tau}$	1.04 ± 0.08	1.00 ± 0.08
$\mathrm{NF}^{\mathrm{VBF_0}}_{Z\to\tau\tau}$	0.95 ± 0.07	1.00 ± 0.08

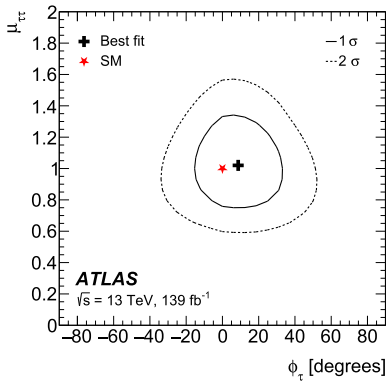

Fig. 6 A 2D likelihood scan of the observed signal strength $\mu_{\tau\tau}$ versus the *CP*-mixing angle ϕ_τ. The 1σ and 2σ confidence regions are shown

Table 7 Impact of different sources of uncertainty on the ϕ_τ measurement

Set of nuisance parameters	Impact on ϕ_τ [degrees]
Jet energy scale	3.4
Jet energy resolution	2.5
Pile-up jet tagging	0.5
Jet flavour tagging	0.2
$E_{\mathrm{T}}^{\mathrm{miss}}$	0.4
Electron	0.3
Muon	0.9
τ_{had} reconstruction	1.0
Misidentified τ	0.6
τ_{had} decay mode classification	0.3
π^0 angular resolution and energy scale	0.2
Track ($\pi^\pm$, impact parameter)	0.7
Luminosity	0.1
Theory uncertainty in $H \to \tau\tau$ processes	1.5
Theory uncertainty in $Z \to \tau\tau$ processes	1.1
Simulated background sample statistics	1.4
Signal normalisation	1.4
Background normalisation	0.6
Total systematic uncertainty	5.2
Data sample statistics	15.6
Total	16.4

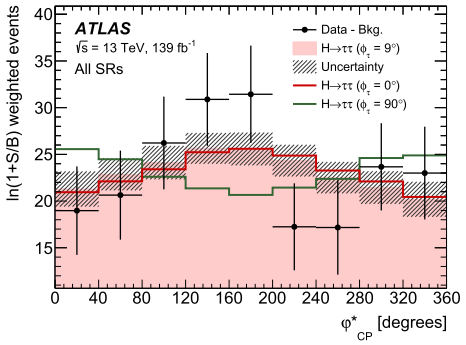

Fig. 7 Combined post-fit distribution of φ^*_{CP} from all signal regions in both the $\tau_{\mathrm{lep}}\,\tau_{\mathrm{had}}$ and $\tau_{\mathrm{had}}\,\tau_{\mathrm{had}}$ channels. Events are weighted with $\ln(1 + S/B)$ for the corresponding signal region. The background is subtracted from data. The best-fit $H \to \tau\tau$ signal is shown in solid pink, while the red and green lines indicate the predictions for the pure *CP*-even (scalar, SM) and pure *CP*-odd (pseudoscalar) hypotheses, respectively, all scaled to the best-fit $H \to \tau\tau$ signal yield. The hatched uncertainty band includes all sources of uncertainty after the fit to data, and represents the same uncertainty in the total signal and background predictions as in Fig. 4

using 139 fb^{-1} of proton–proton collision data recorded at a centre-of-mass energy of $\sqrt{s} = 13$ TeV with the ATLAS detector at the Large Hadron Collider. The measurement is based on a maximum-likelihood fit to the *CP*-sensitive angular observable φ^*_{CP} defined by the visible decay products in the τ_{lep} τ_{had} and τ_{had} τ_{had} decay channels. Depending on the decay channels, different methods are used to reconstruct the φ^*_{CP} distributions. The sensitivity is optimised by applying decay-mode-dependent kinematic selections. The observed (expected) value of $\phi_\tau$is $9° \pm 16°$ ($0° \pm 28°$) at the 68% confidence level, and $\pm 34°$ ($^{+75°}_{-70°}$) at the 2σ level. The pure *CP*-odd hypothesis is disfavoured at a level of 3.4 standard deviations. The analysis precision is limited by the statistical uncertainty of the data sample. The measurement is consistent with the Standard Model expectation.

Acknowledgements We thank CERN for the very successful operation of the LHC, as well as the support staff from our institutions without whom ATLAS could not be operated efficiently. We acknowledge the support of ANPCyT, Argentina; YerPhI, Armenia; ARC, Australia; BMWFW and FWF, Austria; ANAS, Azerbaijan; CNPq and FAPESP, Brazil; NSERC, NRC and CFI, Canada; CERN; ANID, Chile; CAS, MOST and NSFC, China; Minciencias, Colombia; MEYS CR, Czech Republic; DNRF and DNSRC, Denmark; IN2P3-CNRS and CEA-DRF/IRFU, France; SRNSFG, Georgia; BMBF, HGF and MPG, Germany; GSRI, Greece; RGC and Hong Kong SAR, China; ISF and Benoziyo Center, Israel; INFN, Italy; MEXT and JSPS, Japan; CNRST, Morocco; NWO, Netherlands; RCN, Norway; MEiN, Poland; FCT, Portugal; MNE/IFA, Romania; MESTD, Serbia; MSSR, Slovakia; ARRS and MIZŠ, Slovenia; DSI/NRF, South Africa; MICINN, Spain; SRC and Wallenberg Foundation, Sweden; SERI, SNSF and Cantons of Bern and Geneva, Switzerland; MOST, Taiwan; TENMAK, Türkiye; STFC, United Kingdom; DOE and NSF, United States of America. In addition, individual groups and members have received support from BCKDF, CANARIE, Compute Canada and CRC, Canada; PRIMUS 21/SCI/017 and UNCE SCI/013, Czech Republic; COST, ERC, ERDF, Horizon 2020 and Marie Skłodowska-Curie Actions, European Union; Investissements d'Avenir Labex, Investissements d'Avenir Idex and ANR, France; DFG and AvH Foundation, Germany; Herakleitos, Thales and Aristeia programmes co-financed by EU-ESF and the Greek NSRF, Greece; BSF-NSF and MINERVA, Israel; Norwegian Financial Mechanism 2014–2021, Norway; NCN and NAWA, Poland; La Caixa Banking Foundation, CERCA Programme Generalitat de Catalunya and PROMETEO and GenT Programmes Generalitat Valenciana, Spain; Göran Gustafssons Stiftelse, Sweden; The Royal Society and Leverhulme Trust, United Kingdom. The crucial computing support from all WLCG partners is acknowledged gratefully, in particular from CERN, the ATLAS Tier-1 facilities at TRIUMF (Canada), NDGF (Denmark, Norway, Sweden), CC-IN2P3 (France), KIT/GridKA (Germany), INFN-CNAF (Italy), NL-T1 (Netherlands), PIC (Spain), ASGC (Taiwan), RAL (UK) and BNL (USA), the Tier-2 facilities worldwide and large non-WLCG resource providers. Major contributors of computing resources are listed in Ref. [79].

Data Availability Statement This manuscript has no associated data or the data will not be deposited. [Authors' comment: All ATLAS scientific output is published in journals, and preliminary results are made available in Conference Notes. All are openly available, without restriction on use by external parties beyond copyright law and the standard conditions agreed by CERN. Data associated with journal publications are also made available: tables and data from plots (e.g. cross section values, likelihood profiles, selection efficiencies, cross section limits, ...) are stored in appropriate repositories such as HEPDATA (http://hepdata.cedar.ac.uk/). ATLAS also strives to make additional material related to the paper available that allows a reinterpretation of the data in the context of new theoretical models. For example, an extended encapsulation of the analysis is often provided for measurements in the framework of RIVET (http://rivet.hepforge.org/). This information is taken from the ATLAS Data Access Policy, which is a public document that can be downloaded from http://opendata.cern.ch/record/413 [opendata.cern.ch].]

Open Access This article is licensed under a Creative Commons Attribution 4.0 International License, which permits use, sharing, adaptation, distribution and reproduction in any medium or format, as long as you give appropriate credit to the original author(s) and the source, provide a link to the Creative Commons licence, and indicate if changes were made. The images or other third party material in this article are included in the article's Creative Commons licence, unless indicated otherwise in a credit line to the material. If material is not included in the article's Creative Commons licence and your intended use is not permitted by statutory regulation or exceeds the permitted use, you will need to obtain permission directly from the copyright holder. To view a copy of this licence, visit http://creativecommons.org/licenses/by/4.0/.

Funded by SCOAP^3. SCOAP^3 supports the goals of the International Year of Basic Sciences for Sustainable Development.

References

1. ATLAS Collaboration, Evidence for the Higgs-boson Yukawa coupling to tau leptons with the ATLAS detector. JHEP **04**, 117 (2015). https://doi.org/10.1007/JHEP04(2015)117. arXiv:1501.04943 [hep-ex]
2. CMS Collaboration, Evidence for the 125 GeV Higgs boson decaying to a pair of τ leptons. JHEP **05**, 104 (2014). https://doi.org/10.1007/JHEP05(2014)104. arXiv:1401.5041 [hep-ex]
3. ATLAS and CMS Collaborations, Measurements of the Higgs boson production and decay rates and constraints on its couplings from a combined ATLAS and CMS analysis of the LHC pp collision data $\sqrt{s}$ =7 and 8 TeV. JHEP **08**, 045 (2016). https://doi.org/10.1007/JHEP08(2016)045. arXiv:1606.02266 [hep-ex]
4. ATLAS Collaboration, Test of CP Invariance in vector-boson fusion production of the Higgs boson using the Optimal Observable method in the ditau decay channel with the ATLAS detector. Eur. Phys. J. C **76**, 658 (2016). https://doi.org/10.1140/epjc/s10052-016-4499-5. arXiv:1602.04516 [hep-ex]
5. ATLAS Collaboration, Measurement of the Higgs boson coupling properties in the $H \to ZZ^* \to 4l$. decay channel at $\sqrt{s}$=13 TeV with the ATLAS detector. JHEP **03**, 095 (2018). https://doi.org/10.1007/JHEP03(2018)095. arXiv: 1712.02304 [hep-ex]
6. ATLAS Collaboration, Measurements of Higgs boson properties in the diphoton decay channel with $36 fb^{-1}$ of pp collision data at $\sqrt{s}$ = 13 TeV with the ATLAS detector, Phys. Rev. D **98**, 052005 (2018). https://doi.org/10.1103/PhysRevD.98.052005. arXiv:1802.04146 [hep-ex]
7. CMS Collaboration, Combined search for anomalous pseudoscalar HVV couplings in $VH(H \to b\bar{b})$ production and $H \to VV$ decay. Phys. Lett. B **759**, 672 (2016). https://doi.org/10.1016/j.physletb.2016.06.004. arXiv:1602.04305 [hep-ex]
8. CMS Collaboration, Measurements of the Higgs boson width and anomalous HVV couplings from on-shell and off-shell production in the four-lepton final state. Phys. Rev. D **99**, 112003 (2019). https://doi.org/10.1103/PhysRevD.99.112003. arXiv:1901.00174 [hep-ex]

9. CMS Collaboration, Constraints on anomalous HVV couplings from the production of Higgs bosons decaying to τ lepton pairs. Phys. Rev. D **100**, 112002 (2019). https://doi.org/10.1103/PhysRevD.100.112002. arXiv:1903.06973 [hep-ex]
10. C. Zhang, S. Willenbrock, Effective-field-theory approach to top-quark production and decay. Phys. Rev. D **83**, 034006 (2011). https://doi.org/10.1103/PhysRevD.83.034006. arXiv:1008.3869 [hep-ph]
11. ATLAS Collaboration, CP Properties of Higgs boson interactions with top quarks in the $t\bar{t}H$ tH and processes using $H \rightarrow \gamma\gamma$ with the ATLAS detector, Phys. Rev. Lett. **125**, 061802 (2020). https://doi.org/10.1103/PhysRevLett.125.061802. arXiv:2004.04545 [hep-ex]
12. CMS Collaboration, Measurements of $t\bar{t}H$ production and the CP structure of the Yukawa interaction between the Higgs boson and top quark in the diphoton decay channel. Phys. Rev. Lett. **125**, 061801 (2020). https://doi.org/10.1103/PhysRevLett.125.061801. arXiv:2003.10866 [hep-ex]
13. J.R. Dell'Aquila, C.A. Nelson, Useage of the $\bar{\tau}\tau$ or $t\bar{t}$ decay mode to distinguish an intermediate mass Higgs boson from a Technipion. Nucl. Phys. B **320**, 86 (1989). https://doi.org/10.1016/0550-3213(89)90212-5
14. M. Krämer, J.H. Kühn, M.L. Stong, P.M. Zerwas, Prospects of measuring the parity of Higgs particles. Z. Phys. C **64**, 21 (1994). https://doi.org/10.1007/BF01557231. arXiv:hep-ph/9404280
15. G.R. Bower, T. Pierzchala, Z. Was, M. Worek, Measuring the Higgs boson's parity using tau –> rho nu. Phys. Lett. B **543**, 227 (2002). https://doi.org/10.1016/S0370-2693(02)02445-0. arXiv:hep-ph/0204292
16. K. Desch, A. Imhof, Z. Was, M. Worek, Probing the CP nature of the Higgs boson at linear colliders with tau spin correlations: the case of mixed scalar–pseudoscalar couplings. Phys. Lett. B **579**, 157 (2004). https://doi.org/10.1016/j.physletb.2003.10.074. arXiv:hep-ph/0307331
17. S. Berge, W. Bernreuther, H. Spiesberger, Higgs CP properties using the τ decay modes at the ILC. Phys. Lett. B **727**, 488 (2013). https://doi.org/10.1016/j.physletb.2013.11.006. arXiv:1308.2674 [hep-ph]
18. S. Berge, W. Bernreuther, J. Ziethe, Determining the CP parity of Higgs bosons at the LHC in their tau decay channels. Phys. Rev. Lett. **100**, 171605 (2008). https://doi.org/10.1103/PhysRevLett.100.171605. arXiv:0801.2297 [hep-ph]
19. S. Berge, W. Bernreuther, Determining the CP parity of Higgs bosons at the LHC in the tau to 1-prong decay channels. Phys. Lett. B **671**, 470 (2009). https://doi.org/10.1016/j.physletb.2008.12.065. arXiv:0812.1910 [hep-ph]
20. S. Berge, W. Bernreuther, B. Niepelt, H. Spiesberger, How to pin down the CP quantum numbers of a Higgs boson in its tau decays at the LHC. Phys. Rev. D **84**, 116003 (2011). https://doi.org/10.1103/PhysRevD.84.116003. arXiv:1108.0670 [hep-ph]
21. S. Berge, W. Bernreuther, S. Kirchner, Determination of the Higgs CP-mixing angle in the tau decay channels at the LHC including the Drell–Yan background. Eur. Phys. J. C **74**, 3164 (2014). https://doi.org/10.1140/epjc/s10052-014-3164-0. arXiv:1408.0798 [hep-ph]
22. S. Berge, W. Bernreuther, S. Kirchner, Determination of the Higgs CP-mixing angle in the tau decay channels. Nucl. Part. Phys. Proc. **273–275**, 841 (2016). https://doi.org/10.1016/j.nuclphysbps.2015.09.129. arXiv:1410.6362 [hep-ph]
23. S. Berge, W. Bernreuther, S. Kirchner, Prospects of constraining the Higgs boson's CP nature in the tau decay channel at the LHC. Phys. Rev. D **92**, 096012 (2015). https://doi.org/10.1103/PhysRevD.92.096012. arXiv:1510.03850 [hep-ph]
24. CMS Collaboration, Analysis of the CP structure of the Yukawa coupling between the Higgs boson and τ leptons in proton–proton collisions at $\sqrt{s}$ = 13 TeV. JHEP **06**, 012 (2022). https://doi.org/10.1007/JHEP06(2022)012. arXiv:2110.04836 [hep-ex]
25. S. Jadach, Z. Was, Monte Carlo simulation of the process $e^+e^- -> \tau^+\tau^-$, $\tau \rightarrow X^{\pm}$ including radiative O(α^3) QED corrections, mass and spin. Comput. Phys. Commun. **36**, 191 (1985). https://doi.org/10.1016/0010-4655(85)90123-7
26. J.H. Kühn, F. Wagner, Semileptonic decays of the tau lepton. Nucl. Phys. B **236**, 16 (1984). https://doi.org/10.1016/0550-3213(84)90522-4
27. S. Jadach, Z. Was, R. Decker, J.H. Kühn, The tau decay library TAUOLA: version 2.4. Comput. Phys. Commun. **76**, 361 (1993). https://doi.org/10.1016/0010-4655(93)90061-G
28. N. Davidson, G. Nanava, T. Przedzinski, E. Richter-Was, Z. Was, Universal interface of TAUOLA: technical and physics documentation. Comput. Phys. Commun. **183**, 821 (2012). https://doi.org/10.1016/j.cpc.2011.12.009. arXiv:1002.0543 [hep-ph]
29. Y.-S. Tsai, Decay correlations of heavy leptons in e+ e- –> lepton+ lepton−. Phys. Rev. D **4**, 2821 (1971) [Erratum: Phys. Rev. D 13, 771 (1976)]. https://doi.org/10.1103/PhysRevD.13.771
30. Particle Data Group, Review of particle physics. PTEP **2020**, 083C01 (2020). https://doi.org/10.1093/ptep/ptaa104
31. ATLAS Collaboration, The ATLAS experiment at the CERN large hadron collider. JINST **3**, S08003 (2008). https://doi.org/10.1088/1748-0221/3/08/S08003
32. ATLAS Collaboration, ATLAS Insertable B-Layer: Technical Design Report, ATLAS-TDR-19; CERN-LHCC-2010-013 (2010). https://cds.cern.ch/record/1291633 [Addendum: ATLAS-TDR-19-ADD-1; CERN-LHCC-2012-009 (2012). https://cds.cern.ch/record/1451888]
33. B. Abbott et al., Production and integration of the ATLAS Insertable B-Layer. JINST **13**, T05008 (2018). https://doi.org/10.1088/1748-0221/13/05/T05008. arXiv:1803.00844 [physics.ins-det]
34. ATLAS Collaboration, Performance of the ATLAS trigger system in 2015. Eur. Phys. J. C **77**, 317 (2017. https://doi.org/10.1140/epjc/s10052-017-4852-3). arXiv:1611.09661 [hep-ex]
35. ATLAS Collaboration, The ATLAS Collaboration Software and Firmware, ATL-SOFT-PUB-2021-001 (2021). https://cds.cern.ch/record/2767187
36. R. Józefowicz, E. Richter-Was, Z. Was, Potential for optimizing the Higgs boson CP measurement in H $\rightarrow$ $\tau\tau$ decays at the LHC including machine learning techniques. Phys. Rev. D **94**, 093001 (2016). https://doi.org/10.1103/PhysRevD.94.093001. arXiv:1608.02609 [hep-ph]
37. ATLAS Collaboration, ATLAS data quality operations and performance for 2015–2018 data-taking. JINST **15**, P04003 (2020). https://doi.org/10.1088/1748-0221/15/04/P04003. arXiv:1911.04632 [physics.ins-det]
38. ATLAS Collaboration, Performance of electron and photon triggers in ATLAS during LHC Run 2. Eur. Phys. J. C **80**, 47 (2020). https://doi.org/10.1140/epjc/s10052-019-7500-2. arXiv:1909.00761 [hep-ex]
39. ATLAS Collaboration, Performance of the ATLAS muon triggers in Run 2. JINST **15**, P09015 (2020). https://doi.org/10.1088/1748-0221/15/09/p09015. arXiv:2004.13447 [hep-ex]
40. ATLAS Collaboration, The ATLAS Inner Detector Trigger performance in pp collisions at 13 TeV during LHC Run 2. Eur. Phys. J. C **82**, 206 (2021). https://doi.org/10.1140/epjc/s10052-021-09920-0. arXiv:2107.02485 [hep-ex]
41. ATLAS Collaboration, Performance of the ATLAS Level-1 topological trigger in Run 2. Eur. Phys. J. C **82**, 7 (2021). https://doi.org/10.1140/epjc/s10052-021-09807-0. arXiv:2105.01416 [hep-ex]
42. K. Hamilton, P. Nason, E. Re, G. Zanderighi, NNLOPS simulation of Higgs boson production. JHEP **10**, 222 (2013). https://doi.org/10.1007/JHEP10(2013)222. arXiv:1309.0017 [hep-ph]
43. K. Hamilton, P. Nason, G. Zanderighi, Finite quark-mass effects in the NNLOPS POWHEG+MiNLO Higgs generator.

JHEP **05**, 140 (2015). https://doi.org/10.1007/JHEP05(2015)140. arXiv:1501.04637 [hep-ph]
44. S. Alioli, P. Nason, C. Oleari, E. Re, A general framework for implementing NLO calculations in shower Monte Carlo programs: the POWHEG BOX. JHEP **06**, 043 (2010). https://doi.org/10.1007/JHEP06(2010)043. arXiv:1002.2581 [hep-ph]
45. P. Nason, A new method for combining NLO QCD with shower Monte Carlo algorithms. JHEP **11**, 040 (2004). https://doi.org/10.1088/1126-6708/2004/11/040. arXiv:hep-ph/0409146
46. S. Frixione, P. Nason, C. Oleari, Matching NLO QCD computations with Parton Shower simulations: the POWHEG method. JHEP **11**, 070 (2007). https://doi.org/10.1088/1126-6708/2007/11/070. arXiv:0709.2092 [hep-ph]
47. S. Frixione, P. Nason, G. Ridolfi, A positive-weight next-to-leading-order Monte Carlo for heavy flavour hadroproduction. JHEP **09**, 126 (2007). https://doi.org/10.1088/1126-6708/2007/09/126. arXiv:0707.3088 [hep-ph]
48. H.B. Hartanto, B. Jager, L. Reina, D. Wackeroth, Higgs boson production in association with top quarks in the POWHEG BOX. Phys. Rev. D **91**, 094003 (2015). https://doi.org/10.1103/PhysRevD.91.094003. arXiv:1501.04498 [hep-ph]
49. NNPDF Collaboration, R.D. Ball et al., Parton distributions for the LHC Run II. JHEP **04**, 040 (2015). https://doi.org/10.1007/JHEP04(2015)040. arXiv:1410.8849 [hep-ph]
50. T. Sjöstrand et al., An introduction to PYTHIA 8.2. Comput. Phys. Commun. **191**, 159 (2015). https://doi.org/10.1016/j.cpc.2015.01.024. arXiv:1410.3012 [hep-ph]
51. Z. Czyczula, T. Przedzinski, Z. Was, TauSpinner program for studies on spin effect in tau production at the LHC. Eur. Phys. J. C **72**, 1988 (2012). https://doi.org/10.1140/epjc/s10052-012-1988-z. arXiv:1201.0117 [hep-ph]
52. T. Przedzinski, E. Richter-Was, Z. Was, Documentation of TauSpinner algorithms: program for simulating spin effects in τ -lepton production at LHC. Eur. Phys. J. C **79**, 91 (2019). https://doi.org/10.1140/epjc/s10052-018-6527-0. arXiv:1802.05459 [hep-ph]
53. T. Przedzinski, E. Richter-Was, Z. Was, TauSpinner: a tool for simulating CP effects in $H \to \tau\tau$ decays at LHC. Eur. Phys. J. C **74**, 3177 (2014). https://doi.org/10.1140/epjc/s10052-014-3177-8. arXiv:1406.1647 [hep-ph]
54. E. Bothmann et al., Event generation with Sherpa 2.2. SciPost Phys. **7**, 034 (2019). https://doi.org/10.21468/SciPostPhys.7.3.034. arXiv:1905.09127 [hep-ph]
55. ATLAS Collaboration, Measurements of Higgs boson production cross-sections in the $H \to \tau^+\tau^-$ decay channel in pp collisions at $\sqrt{s}$= 13 TeV with the ATLAS detector. JHEP **08**, 175 (2022). https://doi.org/10.1007/JHEP08(2022)175. arXiv:2201.08269 [hep-ex]
56. ATLAS Collaboration, The ATLAS Simulation Infrastructure. Eur. Phys. J. C **70**, 823 (2010). https://doi.org/10.1140/epjc/s10052-010-1429-9. arXiv:1005.4568 [physics.ins-det]
57. GEANT4 Collaboration, S. Agostinelli et al., Geant4-a simulation toolkit. Nucl. Instrum. Meth. A **506**, 250 (2003). https://doi.org/10.1016/S0168-9002(03)01368-8
58. ATLAS Collaboration, Reconstruction of primary vertices at the ATLAS experiment in Run 1 proton-proton collisions at the LHC. Eur. Phys. J. C **77**, 332 (2017). https://doi.org/10.1140/epjc/s10052-017-4887-5. arXiv:1611.10235 [hep-ex]
59. ATLAS Collaboration, Electron and photon performance measurements with the ATLAS detector using the 2015-2017 LHC proton–proton collision data. JINST **14**, P12006 (2019). https://doi.org/10.1088/1748-0221/14/12/P12006. arXiv:1908.00005 [hep-ex]
60. ATLAS Collaboration, Muon reconstruction and identification efficiency in ATLAS using the full Run 2 pp collision data set at $\sqrt{s}$= 13 TeV. Eur. Phys. J. C **81**, 578 (2021). https://doi.org/10.1140/epjc/s10052-021-09233-2. arXiv:2012.00578 [hep-ex]
61. ATLAS Collaboration, Jet reconstruction and performance using particle flow with the ATLAS detector. Eur. Phys. J. C **77**, 466 (2017). https://doi.org/10.1140/epjc/s10052-017-5031-2. arXiv:1703.10485 [hep-ex]
62. M. Cacciari, G.P. Salam, G. Soyez, The anti-k_t jet clustering algorithm. JHEP **04**, 063 (2008). https://doi.org/10.1088/1126-6708/2008/04/063. arXiv:0802.1189 [hep-ph]
63. M. Cacciari, G.P. Salam, G. Soyez, FastJet user manual. Eur. Phys. J. C **72**, 1896 (2012). https://doi.org/10.1140/epjc/s10052-012-1896-2. arXiv:1111.6097 [hep-ph]
64. ATLAS Collaboration, Selection of jets produced in 13 TeV proton–proton collisions with the ATLAS detector, ATLAS-CONF-2015-029 (2015). https://cds.cern.ch/record/2037702
65. ATLAS Collaboration, Performance of pile-up mitigation techniques for jets in pp collisions at $\sqrt{s}$= 8 TeV using the ATLAS detector. Eur. Phys. J. C **76**, 581 (2016). https://doi.org/10.1140/epjc/s10052-016-4395-z. arXiv:1510.03823 [hep-ex]
66. ATLAS Collaboration, Identification and rejection of pile-up jets at high pseudorapidity with the ATLAS detector. Eur. Phys. J. C **77**, 580 (2017) [Erratum: Eur. Phys. J. C 77 (2017) 712]. https://doi.org/10.1140/epjc/s10052-017-5081-5. arXiv:1705.02211 [hep-ex]
67. ATLAS Collaboration, Topological cell clustering in the ATLAS calorimeters and its performance in LHC Run 1. Eur. Phys. J. C **77**, 490 (2017). https://doi.org/10.1140/epjc/s10052-017-5004-5. arXiv:1603.02934 [hep-ex]
68. ATLAS Collaboration, Measurement of the tau lepton reconstruction and identification performance in the ATLAS experiment using pp collisions at $\sqrt{s}$ = 13 TeV, ATLAS-CONF-2017-029 (2017). https://cds.cern.ch/record/2261772
69. ATLAS Collaboration, Identification of hadronic tau lepton decays using neural networks in the ATLAS experiment, ATL-PHYS-PUB-2019-033 (2019). https://cds.cern.ch/record/2688062
70. ATLAS Collaboration, Performance of missing transverse momentum reconstruction with the ATLAS detector using proton–proton collisions at $\sqrt{s}$ = 13 TeV. Eur. Phys. J. C **78**, 903 (2018). https://doi.org/10.1140/epjc/s10052-018-6288-9. arXiv:1802.08168 [hep-ex]
71. A. Elagin, P. Murat, A. Pranko, A. Safonov, A new mass reconstruction technique for resonances decaying to di-tau. Nucl. Instrum. Meth. A **654**, 481 (2011). https://doi.org/10.1016/j.nima.2011.07.009. arXiv:1012.4686 [hep-ex]
72. ATLAS Collaboration, Reconstruction of hadronic decay products of tau leptons with the ATLAS experiment. Eur. Phys. J. C **76**, 295 (2016). https://doi.org/10.1140/epjc/s10052-016-4110-0. arXiv:1512.05955 [hep-ex]
73. The new LUCID-2 detector for luminosity measurement and monitoring in ATLAS. JINST **13**(07), P07017 (2018). https://doi.org/10.1088/1748-0221/13/07/P07017
74. ATLAS Collaboration, Luminosity determination in pp collisions at $\sqrt{s}$ = 13 TeV using the ATLAS detector at the LHC, ATLAS-CONF-2019-021 (2019). https://cds.cern.ch/record/2677054
75. ATLAS Collaboration, Jet energy scale and resolution measured in proton-proton collisions at $\sqrt{s}$ = 13 TeV with the ATLAS detector. Eur. Phys. J. C **81**, 689 (2020). https://doi.org/10.1140/epjc/s10052-021-09402-3. arXiv:2007.02645 [hep-ex]
76. ATLAS Collaboration, Cross-section measurements of the Higgs boson decaying into a pair of τ-leptons in proton-proton collisions at $\sqrt{s}$ = 13 TeV with the ATLAS detector. Phys. Rev. D **99**, 072001 (2019). https://doi.org/10.1103/PhysRevD.99.072001. arXiv:1811.08856 [hep-ex]
77. ATLAS Collaboration, Measurement of the energy response of the ATLAS calorimeter to charged pions from $W^\pm \to \tau^\pm(\to \pi^\pm \nu_\tau)\nu_\tau$ events in Run 2 data. Eur. Phys. J. C **82**, 223 (2021). https://doi.org/10.1140/epjc/s10052-022-10117-2. arXiv:2108.09043 [hep-ex]

ATLAS Collaboration[★]

G. Aad[101], B. Abbott[119], D. C. Abbott[102], K. Abeling[55], S. H. Abidi[29], A. Aboulhorma[35e], H. Abramowicz[150], H. Abreu[149], Y. Abulaiti[116], A. C. Abusleme Hoffman[136a], B. S. Acharya[68a,68b,o], B. Achkar[55], C. Adam Bourdarios[4], L. Adamczyk[84a], L. Adamek[154], S. V. Addepalli[26], J. Adelman[114], A. Adiguzel[21c], S. Adorni[56], T. Adye[133], A. A. Affolder[135], Y. Afik[36], M. N. Agaras[13], J. Agarwala[72a,72b], A. Aggarwal[99], C. Agheorghiesei[27c], J. A. Aguilar-Saavedra[129f], A. Ahmad[36], F. Ahmadov[38,w], W. S. Ahmed[103], S. Ahuja[94], X. Ai[48], G. Aielli[75a,75b], I. Aizenberg[168], M. Akbiyik[99], T. P. A. Åkesson[97], A. V. Akimov[37], K. Al Khoury[41], G. L. Alberghi[23b], J. Albert[164], P. Albicocco[53], M. J. Alconada Verzini[89], S. Alderweireldt[52], M. Aleksa[36], I. N. Aleksandrov[38], C. Alexa[27b], T. Alexopoulos[10], A. Alfonsi[113], F. Alfonsi[23b], M. Alhroob[119], B. Ali[131], S. Ali[147], M. Aliev[37], G. Alimonti[70a], W. Alkakhi[55], C. Allaire[36], B. M. M. Allbrooke[145], P. P. Allport[20], A. Aloisio[71a,71b], F. Alonso[89], C. Alpigiani[137], E. Alunno Camelia[75a,75b], M. Alvarez Estevez[98], M. G. Alviggi[71a,71b], Y. Amaral Coutinho[81b], A. Ambler[103], C. Amelung[36], C. G. Ames[108], D. Amidei[105], S. P. Amor Dos Santos[129a], S. Amoroso[48], K. R. Amos[162], C. S. Amrouche[56], V. Ananiev[124], C. Anastopoulos[138], T. Andeen[11], J. K. Anders[19], S. Y. Andrean[47a,47b], A. Andreazza[70a,70b], S. Angelidakis[9], A. Angerami[41,y], A. V. Anisenkov[37], A. Annovi[73a], C. Antel[56], M. T. Anthony[138], E. Antipov[120], M. Antonelli[53], D. J. A. Antrim[17a], F. Anulli[74a], M. Aoki[82], T. Aoki[152], J. A. Aparisi Pozo[162], M. A. Aparo[145], L. Aperio Bella[48], C. Appelt[18], N. Aranzabal[36], V. Araujo Ferraz[81a], C. Arcangeletti[53], A. T. H. Arce[51], E. Arena[91], J.-F. Arguin[107], S. Argyropoulos[54], J. -H. Arling[48], A. J. Armbruster[36], O. Arnaez[154], H. Arnold[113], Z. P. Arrubarrena Tame[108], G. Artoni[74a,74b], H. Asada[110], K. Asai[117], S. Asai[152], N. A. Asbah[61], J. Assahsah[35d], K. Assamagan[29], R. Astalos[28a], R. J. Atkin[33a], M. Atkinson[161], N. B. Atlay[18], H. Atmani[62b], P. A. Atmasiddha[105], K. Augsten[131], S. Auricchio[71a,71b], A. D. Auriol[20], V. A. Austrup[170], G. Avner[149], G. Avolio[36], K. Axiotis[56], M. K. Ayoub[14c], G. Azuelos[107,aa], D. Babal[28a], H. Bachacou[134], K. Bachas[151,q], A. Bachiu[34], F. Backman[47a,47b], A. Badea[61], P. Bagnaia[74a,74b], M. Bahmani[18], A. J. Bailey[162], V. R. Bailey[161], J. T. Baines[133], C. Bakalis[10], O. K. Baker[171], P. J. Bakker[113], E. Bakos[15], D. Bakshi Gupta[8], S. Balaji[146], R. Balasubramanian[113], E. M. Baldin[37], P. Balek[132], E. Ballabene[70a,70b], F. Balli[134], L. M. Baltes[63a], W. K. Balunas[32], J. Balz[99], E. Banas[85], M. Bandieramonte[128], A. Bandyopadhyay[24], S. Bansal[24], L. Barak[150], E. L. Barberio[104], D. Barberis[57a,57b], M. Barbero[101], G. Barbour[95], K. N. Barends[33a], T. Barillari[109], M.-S. Barisits[36], T. Barklow[142], R. M. Barnett[17a], P. Baron[121], D. A. Baron Moreno[100], A. Baroncelli[62a], G. Barone[29], A. J. Barr[125], L. Barranco Navarro[47a,47b], F. Barreiro[98], J. Barreiro Guimarães da Costa[14a], U. Barron[150], M. G. Barros Teixeira[129a], S. Barsov[37], F. Bartels[63a], R. Bartoldus[142], A. E. Barton[90], P. Bartos[28a], A. Basalaev[48], A. Basan[99], M. Baselga[49], I. Bashta[76a,76b], A. Bassalat[66,ag], M. J. Basso[154], C. R. Basson[100], R. L. Bates[59], S. Batlamous[35e], J. R. Batley[32], B. Batool[140], M. Battaglia[135], D. Battulga[18], M. Bauce[74a,74b], P. Bauer[24], A. Bayirli[21a], J. B. Beacham[51], T. Beau[126], P. H. Beauchemin[157], F. Beche rer[54], P. Bechtle[24], H. P. Beck[19,p], K. Becker[166], C. Becot[48], A. J. Beddall[21d], V. A. Bednyakov[38], C. P. Bee[144], L. J. Beemster[15], T. A. Beermann[36], M. Begalli[81d], M. Begel[29], A. Behera[144], J. K. Behr[48], C. Beirao Da Cruz E Silva[36], J. F. Beirer[36,55], F. Beisiegel[24], M. Belfkir[158], G. Bella[150], L. Bellagamba[23b], A. Bellerive[34], P. Bellos[20], K. Beloborodov[37], K. Belotskiy[37], N. L. Belyaev[37], D. Benchekroun[35a], F. Bendebba[35a], Y. Benhammou[150], D. P. Benjamin[29], M. Benoit[29], J. R. Bensinger[26], S. Bentvelsen[113], L. Beresford[36], M. Beretta[53], D. Berge[18], E. Bergeaas Kuutmann[160], N. Berger[4], B. Bergmann[131], J. Beringer[17a], S. Berlendis[7], G. Bernardi[5], C. Bernius[142], F. U. Bernlochner[24], T. Berry[94], P. Berta[132], A. Berthold[50], I. A. Bertram[90], S. Bethke[109], A. Betti[74a,74b], A. J. Bevan[93], M. Bhamjee[33c], S. Bhatta[144], D. S. Bhattacharya[165], P. Bhattarai[26], V. S. Bhopatkar[120], R. Bi[29,ad], R. M. Bianchi[128], O. Biebel[108], R. Bielski[122], M. Biglietti[76a], T. R. V. Billoud[131], M. Bindi[55], A. Bingul[21b], C. Bini[74a,74b], S. Biondi[23a,23b], A. Biondini[91], C. J. Birch-sykes[100], G. A. Bird[20,133], M. Birman[168], T. Bisanz[36], E. Bisceglie[43a,43b], D. Biswas[169,k], A. Bitadze[100], K. Bjørke[124], I. Bloch[48], C. Blocker[26], A. Blue[59], U. Blumenschein[93], J. Blumenthal[99], G. J. Bobbink[113], V. S. Bobrovnikov[37], M. Boehler[54], D. Bogavac[36], A. G. Bogdanchikov[37], C. Bohm[47a], V. Boisvert[94], P. Bokan[48], T. Bold[84a], M. Bomben[5], M. Bona[93], M. Boonekamp[134], C. D. Booth[94], A. G. Borbély[59], H. M. Borecka-Bielska[107], L. S. Borgna[95], G. Borissov[90], D. Bortoletto[125], D. Boscherini[23b], M. Bosman[13], J. D. Bossio Sola[36], K. Bouaouda[35a], J. Boudreau[128], E. V. Bouhova-Thacker[90], D. Boumediene[40], R. Bouquet[5], A. Boveia[118], J. Boyd[36], D. Boye[29], I. R. Boyko[38], J. Bracinik[20], N. Brahimi[62d], G. Brandt[170], O. Brandt[32], F. Braren[48], B. Brau[102],

J. E. Brau[122], K. Brendlinger[48], R. Brener[168], L. Brenner[36], R. Brenner[160], S. Bressler[168], B. Brickwedde[99], D. Britton[59], D. Britzger[109], I. Brock[24], G. Brooijmans[41], W. K. Brooks[136f], E. Brost[29], T. L. Bruckler[125], P. A. Bruckman de Renstrom[85], B. Brüers[48], D. Bruncko[28b,*], A. Bruni[23b], G. Bruni[23b], M. Bruschi[23b], N. Bruscino[74a,74b], L. Bryngemark[142], T. Buanes[16], Q. Buat[137], P. Buchholz[140], A. G. Buckley[59], I. A. Budagov[38,*], M. K. Bugge[124], O. Bulekov[37], B. A. Bullard[61], S. Burdin[91], C. D. Burgard[48], A. M. Burger[40], B. Burghgrave[8], J. T. P. Burr[32], C. D. Burton[11], J. C. Burzynski[141], E. L. Busch[41], V. Büscher[99], P. J. Bussey[59], J. M. Butler[25], C. M. Buttar[59], J. M. Butterworth[95], W. Buttinger[133], C. J. Buxo Vazquez[106], A. R. Buzykaev[37], G. Cabras[23b], S. Cabrera Urbán[162], D. Caforio[58], H. Cai[128], Y. Cai[14a,14d], V. M. M. Cairo[36], O. Cakir[3a], N. Calace[36], P. Calafiura[17a], G. Calderini[126], P. Calfayan[67], G. Callea[59], L. P. Caloba[81b], D. Calvet[40], S. Calvet[40], T. P. Calvet[101], M. Calvetti[73a,73b], R. Camacho Toro[126], S. Camarda[36], D. Camarero Munoz[26], P. Camarri[75a,75b], M. T. Camerlingo[76a,76b], D. Cameron[124], C. Camincher[164], M. Campanelli[95], A. Camplani[42], V. Canale[71a,71b], A. Canesse[103], M. Cano Bret[79], J. Cantero[162], Y. Cao[161], F. Capocasa[26], M. Capua[43a,43b], A. Carbone[70a,70b], R. Cardarelli[75a], J. C. J. Cardenas[8], F. Cardillo[162], T. Carli[36], G. Carlino[71a], J. I. Carlotto[13], B. T. Carlson[128,r], E. M. Carlson[155a,164], L. Carminati[70a,70b], M. Carnesale[74a,74b], S. Caron[112], E. Carquin[136f], S. Carrá[70a,70b], G. Carratta[23a,23b], F. Carrio Argos[33g], J. W. S. Carter[154], T. M. Carter[52], M. P. Casado[13,h], A. F. Casha[154], E. G. Castiglia[171], F. L. Castillo[63a], L. Castillo Garcia[13], V. Castillo Gimenez[162], N. F. Castro[129a,129e], A. Catinaccio[36], J. R. Catmore[124], V. Cavaliere[29], N. Cavalli[23a,23b], V. Cavasinni[73a,73b], E. Celebi[21a], F. Celli[125], M. S. Centonze[69a,69b], K. Cerny[121], A. S. Cerqueira[81a], A. Cerri[145], L. Cerrito[75a,75b], F. Cerutti[17a], A. Cervelli[23b], S. A. Cetin[21d], Z. Chadi[35a], D. Chakraborty[114], M. Chala[129f], J. Chan[169], W. Y. Chan[152], J. D. Chapman[32], B. Chargeishvili[148b], D. G. Charlton[20], T. P. Charman[93], M. Chatterjee[19], S. Chekanov[6], S. V. Chekulaev[155a], G. A. Chelkov[38,a], A. Chen[105], B. Chen[150], B. Chen[164], C. Chen[62a], H. Chen[14c], H. Chen[29], J. Chen[62c], J. Chen[26], S. Chen[152], S. J. Chen[14c], X. Chen[62c], X. Chen[14b,z], Y. Chen[62a], C. L. Cheng[169], H. C. Cheng[64a], A. Cheplakov[38], E. Cheremushkina[48], E. Cherepanova[113], R. Cherkaoui El Moursli[35e], E. Cheu[7], K. Cheung[65], L. Chevalier[134], V. Chiarella[53], G. Chiarelli[73a], N. Chiedde[101], G. Chiodini[69a], A. S. Chisholm[20], A. Chitan[27b], M. Chitishvili[162], Y. H. Chiu[164], M. V. Chizhov[38], K. Choi[11], A. R. Chomont[74a,74b], Y. Chou[102], E. Y. S. Chow[113], T. Chowdhury[33g], L. D. Christopher[33g], K. L. Chu[64a], M. C. Chu[64a], X. Chu[14a,14d], J. Chudoba[130], J. J. Chwastowski[85], D. Cieri[109], K. M. Ciesla[84a], V. Cindro[92], A. Ciocio[17a], F. Cirotto[71a,71b], Z. H. Citron[168,l], M. Citterio[70a], D. A. Ciubotaru[27b], B. M. Ciungu[154], A. Clark[56], P. J. Clark[52], J. M. Clavijo Columbie[48], S. E. Clawson[100], C. Clement[47a,47b], J. Clercx[48], L. Clissa[23a,23b], Y. Coadou[101], M. Cobal[68a,68c], A. Coccaro[57b], R. F. Coelho Barrue[129a], R. Coelho Lopes De Sa[102], S. Coelli[70a], H. Cohen[150], A. E. C. Coimbra[70a,70b], B. Cole[41], J. Collot[60], P. Conde Muiño[129a,129g], M. P. Connell[33c], S. H. Connell[33c], I. A. Connelly[59], E. I. Conroy[125], F. Conventi[71a,ab], H. G. Cooke[20], A. M. Cooper-Sarkar[125], F. Cormier[163], L. D. Corpe[36], M. Corradi[74a,74b], E. E. Corrigan[97], F. Corriveau[103,v], A. Cortes-Gonzalez[18], M. J. Costa[162], F. Costanza[4], D. Costanzo[138], B. M. Cote[118], G. Cowan[94], J. W. Cowley[32], K. Cranmer[116], S. Crépé-Renaudin[60], F. Crescioli[126], M. Cristinziani[140], M. Cristoforetti[77a,77b,c], V. Croft[157], G. Crosetti[43a,43b], A. Cueto[36], T. Cuhadar Donszelmann[159], H. Cui[14a,14d], Z. Cui[7], A. R. Cukierman[142], W. R. Cunningham[59], F. Curcio[43a,43b], P. Czodrowski[36], M. M. Czurylo[63b], M. J. Da Cunha Sargedas De Sousa[62a], J. V. Da Fonseca Pinto[81b], C. Da Via[100], W. Dabrowski[84a], T. Dado[49], S. Dahbi[33g], T. Dai[105], C. Dallapiccola[102], M. Dam[42], G. D'amen[29], V. D'Amico[108], J. Damp[99], J. R. Dandoy[127], M. F. Daneri[30], M. Danninger[141], V. Dao[36], G. Darbo[57b], S. Darmora[6], S. J. Das[29], S. D'Auria[70a,70b], C. David[155b], T. Davidek[132], D. R. Davis[51], B. Davis-Purcell[34], I. Dawson[93], K. De[8], R. De Asmundis[71a], M. De Beurs[113], N. De Biase[48], S. De Castro[23a,23b], N. De Groot[112], P. de Jong[113], H. De la Torre[106], A. De Maria[14c], A. De Salvo[74a], U. De Sanctis[75a,75b], A. De Santo[145], J. B. De Vivie De Regie[60], D. V. Dedovich[38], J. Degens[113], A. M. Deiana[44], F. Del Corso[23a,23b], J. Del Peso[98], F. Del Rio[63a], F. Deliot[134], C. M. Delitzsch[49], M. Della Pietra[71a,71b], D. Della Volpe[56], A. Dell'Acqua[36], L. Dell'Asta[70a,70b], M. Delmastro[4], P. A. Delsart[60], S. Demers[171], M. Demichev[38], S. P. Denisov[37], L. D'Eramo[114], D. Derendarz[85], F. Derue[126], P. Dervan[91], K. Desch[24], K. Dette[154], C. Deutsch[24], P. O. Deviveiros[36], F. A. Di Bello[74a,74b], A. Di Ciaccio[75a,75b], L. Di Ciaccio[4], A. Di Domenico[74a,74b], C. Di Donato[71a,71b], A. Di Girolamo[36], G. Di Gregorio[73a,73b], A. Di Luca[77a,77b], B. Di Micco[76a,76b], R. Di Nardo[76a,76b], C. Diaconu[101], F. A. Dias[113], T. Dias Do Vale[141], M. A. Diaz[136a,136b], F. G. Diaz Capriles[24], M. Didenko[162], E. B. Diehl[105], L. Diehl[54], S. Díez Cornell[48], C. Diez Pardos[140], C. Dimitriadi[24,160], A. Dimitrievska[17a],

W. Ding[14b], J. Dingfelder[24], I.-M. Dinu[27b], S. J. Dittmeier[63b], F. Dittus[36], F. Djama[101], T. Djobava[148b], J. I. Djuvsland[16], C. Doglioni[97,100], J. Dolejsi[132], Z. Dolezal[132], M. Donadelli[81c], B. Dong[62c], J. Donini[40], A. D'Onofrio[14c], M. D'Onofrio[91], J. Dopke[133], A. Doria[71a], M. T. Dova[89], A. T. Doyle[59], M. A. Draguet[125], E. Drechsler[141], E. Dreyer[168], I. Drivas-koulouris[10], A. S. Drobac[157], M. Drozdova[56], D. Du[62a], T. A. du Pree[113], F. Dubinin[37], M. Dubovsky[28a], E. Duchovni[168], G. Duckeck[108], O. A. Ducu[27b], D. Duda[109], A. Dudarev[36], M. D'uffizi[100], L. Duflot[66], M. Dührssen[36], C. Dülsen[170], A. E. Dumitriu[27b], M. Dunford[63a], S. Dungs[49], K. Dunne[47a,47b], A. Duperrin[101], H. Duran Yildiz[3a], M. Düren[58], A. Durglishvili[148b], B. L. Dwyer[114], G. I. Dyckes[17a], M. Dyndal[84a], S. Dysch[100], B. S. Dziedzic[85], Z. O. Earnshaw[145], B. Eckerova[28a], M. G. Eggleston[51], E. Egidio Purcino De Souza[81b], L. F. Ehrke[56], G. Eigen[16], K. Einsweiler[17a], T. Ekelof[160], P. A. Ekman[97], Y. El Ghazali[35b], H. El Jarrari[35e,147], A. El Moussaouy[35a], V. Ellajosyula[160], M. Ellert[160], F. Ellinghaus[170], A. A. Elliot[93], N. Ellis[36], J. Elmsheuser[29], M. Elsing[36], D. Emeliyanov[133], A. Emerman[41], Y. Enari[152], I. Ene[17a], S. Epari[13], J. Erdmann[49], A. Ereditato[19], P. A. Erland[85], M. Errenst[170], M. Escalier[66], C. Escobar[162], E. Etzion[150], G. Evans[129a], H. Evans[67], M. O. Evans[145], A. Ezhilov[37], S. Ezzarqtouni[35a], F. Fabbri[59], L. Fabbri[23a,23b], G. Facini[95], V. Fadeyev[135], R. M. Fakhrutdinov[37], S. Falciano[74a], P. J. Falke[24], S. Falke[36], J. Faltova[132], Y. Fan[14a], Y. Fang[14a,14d], G. Fanourakis[46], M. Fanti[70a,70b], M. Faraj[68a,68b], A. Farbin[8], A. Farilla[76a], T. Farooque[106], S. M. Farrington[52], F. Fassi[35e], D. Fassouliotis[9], M. Faucci Giannelli[75a,75b], W. J. Fawcett[32], L. Fayard[66], P. Federicova[130], O. L. Fedin[37,a], G. Fedotov[37], M. Feickert[161], L. Feligioni[101], A. Fell[138], D. E. Fellers[122], C. Feng[62b], M. Feng[14b], Z. Feng[113], M. J. Fenton[159], A. B. Fenyuk[37], L. Ferencz[48], S. W. Ferguson[45], J. Ferrando[48], A. Ferrari[160], P. Ferrari[113], R. Ferrari[72a], D. Ferrere[56], C. Ferretti[105], F. Fiedler[99], A. Filipčič[92], E. K. Filmer[1], F. Filthaut[112], M. C. N. Fiolhais[129a,129c,b], L. Fiorini[162], F. Fischer[140], W. C. Fisher[106], T. Fitschen[20], I. Fleck[140], P. Fleischmann[105], T. Flick[170], L. Flores[127], M. Flores[33d], L. R. Flores Castillo[64a], F. M. Follega[77a,77b], N. Fomin[16], J. H. Foo[154], B. C. Forland[67], A. Formica[134], A. C. Forti[100], E. Fortin[101], A. W. Fortman[61], M. G. Foti[17a], L. Fountas[9], D. Fournier[66], H. Fox[90], P. Francavilla[73a,73b], S. Francescato[61], M. Franchini[23a,23b], S. Franchino[63a], D. Francis[36], L. Franco[112], L. Franconi[19], M. Franklin[61], G. Frattari[26], A. C. Freegard[93], P. M. Freeman[20], W. S. Freund[81b], N. Fritzsche[50], A. Froch[54], D. Froidevaux[36], J. A. Frost[125], Y. Fu[62a], M. Fujimoto[117], E. Fullana Torregrosa[162,*], J. Fuster[162], A. Gabrielli[23a,23b], A. Gabrielli[154], P. Gadow[48], G. Gagliardi[57a,57b], L. G. Gagnon[17a], G. E. Gallardo[125], E. J. Gallas[125], B. J. Gallop[133], R. Gamboa Goni[93], K. K. Gan[118], S. Ganguly[152], J. Gao[62a], Y. Gao[52], F. M. Garay Walls[136a,136b], B. Garcia[29,ad], C. García[162], J. E. García Navarro[162], J. A. García Pascual[14a], M. Garcia-Sciveres[17a], R. W. Gardner[39], D. Garg[79], R. B. Garg[142], S. Gargiulo[54], C. A. Garner[154], V. Garonne[29], S. J. Gasiorowski[137], P. Gaspar[81b], G. Gaudio[72a], V. Gautam[13], P. Gauzzi[74a,74b], I. L. Gavrilenko[37], A. Gavrilyuk[37], C. Gay[163], G. Gaycken[48], E. N. Gazis[10], A. A. Geanta[27b,27e], C. M. Gee[135], J. Geisen[97], M. Geisen[99], C. Gemme[57b], M. H. Genest[60], S. Gentile[74a,74b], S. George[94], W. F. George[20], T. Geralis[46], L. O. Gerlach[55], P. Gessinger-Befurt[36], M. Ghasemi Bostanabad[164], M. Ghneimat[140], A. Ghosal[140], A. Ghosh[159], A. Ghosh[7], B. Giacobbe[23b], S. Giagu[74a,74b], N. Giangiacomi[154], P. Giannetti[73a], A. Giannini[62a], S. M. Gibson[94], M. Gignac[135], D. T. Gil[84b], A. K. Gilbert[84a], B. J. Gilbert[41], D. Gillberg[34], G. Gilles[113], N. E. K. Gillwald[48], L. Ginabat[126], D. M. Gingrich[2,aa], M. P. Giordani[68a,68c], P. F. Giraud[134], G. Giugliarelli[68a,68c], D. Giugni[70a], F. Giuli[36], I. Gkialas[9,i], L. K. Gladilin[37], C. Glasman[98], G. R. Gledhill[122], M. Glisic[122], I. Gnesi[43b,e], Y. Go[29,ad], M. Goblirsch-Kolb[26], D. Godin[107], S. Goldfarb[104], T. Golling[56], M. G. D. Gololo[33g], D. Golubkov[37], J. P. Gombas[106], A. Gomes[129a,129b], G. Gomes Da Silva[140], A. J. Gomez Delegido[162], R. Goncalves Gama[55], R. Gonçalo[129a,129c], G. Gonella[122], L. Gonella[20], A. Gongadze[38], F. Gonnella[20], J. L. Gonski[41], R. Y. González Andana[52], S. González de la Hoz[162], S. Gonzalez Fernandez[13], R. Gonzalez Lopez[91], C. Gonzalez Renteria[17a], R. Gonzalez Suarez[160], S. Gonzalez-Sevilla[56], G. R. Gonzalvo Rodriguez[162], L. Goossens[36], N. A. Gorasia[20], P. A. Gorbounov[37], B. Gorini[36], E. Gorini[69a,69b], A. Gorišek[92], A. T. Goshaw[51], M. I. Gostkin[38], C. A. Gottardo[36], M. Gouighri[35b], V. Goumarre[48], A. G. Goussiou[137], N. Govender[33c], C. Goy[4], I. Grabowska-Bold[84a], K. Graham[34], E. Gramstad[124], S. Grancagnolo[18], M. Grandi[145], V. Gratchev[37,*], P. M. Gravila[27f], F. G. Gravili[69a,69b], H. M. Gray[17a], M. Greco[69a,69b], C. Grefe[24], I. M. Gregor[48], P. Grenier[142], C. Grieco[13], A. A. Grillo[135], K. Grimm[31,m], S. Grinstein[13,t], J. -F. Grivaz[66], E. Gross[168], J. Grosse-Knetter[55], C. Grud[105], A. Grummer[111], J. C. Grundy[125], L. Guan[105], W. Guan[169], C. Gubbels[163], J. G. R. Guerrero Rojas[162], G. Guerrieri[68a,68b], F. Guescini[109], R. Gugel[99], J. A. M. Guhit[105], A. Guida[48], T. Guillemin[4], E. Guilloton[133,166], S. Guindon[36], F. Guo[14a,14d], J. Guo[62c],

L. Guo[66], Y. Guo[105], R. Gupta[48], S. Gurbuz[24], S. S. Gurdasani[54], G. Gustavino[36], M. Guth[56], P. Gutierrez[119], L. F. Gutierrez Zagazeta[127], C. Gutschow[95], C. Guyot[134], C. Gwenlan[125], C. B. Gwilliam[91], E. S. Haaland[124], A. Haas[116], M. Habedank[48], C. Haber[17a], H. K. Hadavand[8], A. Hadef[99], S. Hadzic[109], M. Haleem[165], J. Haley[120], J. J. Hall[138], G. D. Hallewell[101], L. Halser[19], K. Hamano[164], H. Hamdaoui[35e], M. Hamer[24], G. N. Hamity[52], J. Han[62b], K. Han[62a], L. Han[14c], L. Han[62a], S. Han[17a], Y. F. Han[154], K. Hanagaki[82], M. Hance[135], D. A. Hangal[41,y], H. Hanif[141], M. D. Hank[39], R. Hankache[100], J. B. Hansen[42], J. D. Hansen[42], P. H. Hansen[42], K. Hara[156], D. Harada[56], T. Harenberg[170], S. Harkusha[37], Y. T. Harris[125], N. M. Harrison[118], P. F. Harrison[166], N. M. Hartman[142], N. M. Hartmann[108], Y. Hasegawa[139], A. Hasib[52], S. Haug[19], R. Hauser[106], M. Havranek[131], C. M. Hawkes[20], R. J. Hawkings[36], S. Hayashida[110], D. Hayden[106], C. Hayes[105], R. L. Hayes[163], C. P. Hays[125], J. M. Hays[93], H. S. Hayward[91], F. He[62a], Y. He[153], Y. He[126], M. P. Heath[52], V. Hedberg[97], A. L. Heggelund[124], N. D. Hehir[93], C. Heidegger[54], K. K. Heidegger[54], W. D. Heidorn[80], J. Heilman[34], S. Heim[48], T. Heim[17a], J. G. Heinlein[127], J. J. Heinrich[122], L. Heinrich[109], J. Hejbal[130], L. Helary[48], A. Held[169], S. Hellesund[124], C. M. Helling[163], S. Hellman[47a,47b], C. Helsens[36], R. C. W. Henderson[90], L. Henkelmann[32], A. M. Henriques Correia[36], H. Herde[142], Y. Hernández Jiménez[144], M. G. Herrmann[108], T. Herrmann[50], G. Herten[54], R. Hertenberger[108], L. Hervas[36], N. P. Hessey[155a], H. Hibi[83], E. Higón-Rodriguez[162], S. J. Hillier[20], I. Hinchliffe[17a], F. Hinterkeuser[24], M. Hirose[123], S. Hirose[156], D. Hirschbuehl[170], T. G. Hitchings[100], B. Hiti[92], J. Hobbs[144], R. Hobincu[27e], N. Hod[168], M. C. Hodgkinson[138], B. H. Hodkinson[32], A. Hoecker[36], J. Hofer[48], D. Hohn[54], T. Holm[24], M. Holzbock[109], L. B. A. H. Hommels[32], B. P. Honan[100], J. Hong[62c], T. M. Hong[128], Y. Hong[55], J. C. Honig[54], A. Hönle[109], B. H. Hooberman[161], W. H. Hopkins[6], Y. Horii[110], S. Hou[147], A. S. Howard[92], J. Howarth[59], J. Hoya[6], M. Hrabovsky[121], A. Hrynevich[37], T. Hryn'ova[4], P. J. Hsu[65], S. -C. Hsu[137], Q. Hu[41,y], Y. F. Hu[14a,14d,ac], D. P. Huang[95], S. Huang[64b], X. Huang[14c], Y. Huang[62a], Y. Huang[14a], Z. Huang[100], Z. Hubacek[131], M. Huebner[24], F. Huegging[24], T. B. Huffman[125], M. Huhtinen[36], S. K. Huiberts[16], R. Hulsken[103], N. Huseynov[12,a], J. Huston[106], J. Huth[61], R. Hyneman[142], S. Hyrych[28a], G. Iacobucci[56], G. Iakovidis[29], I. Ibragimov[140], L. Iconomidou-Fayard[66], P. Iengo[71a,71b], R. Iguchi[152], T. Iizawa[56], Y. Ikegami[82], A. Ilg[19], N. Ilic[154], H. Imam[35a], T. Ingebretsen Carlson[47a,47b], G. Introzzi[72a,72b], M. Iodice[76a], V. Ippolito[74a,74b], M. Ishino[152], W. Islam[169], C. Issever[18,48], S. Istin[21a,af], H. Ito[167], J. M. Iturbe Ponce[64a], R. Iuppa[77a,77b], A. Ivina[168], J. M. Izen[45], V. Izzo[71a], P. Jacka[130,131], P. Jackson[1], R. M. Jacobs[48], B. P. Jaeger[141], C. S. Jagfeld[108], G. Jäkel[170], K. Jakobs[54], T. Jakoubek[168], J. Jamieson[59], K. W. Janas[84a], G. Jarlskog[97], A. E. Jaspan[91], M. Javurkova[102], F. Jeanneau[134], L. Jeanty[122], J. Jejelava[148a,x], P. Jenni[54,f], C. E. Jessiman[34], S. Jézéquel[4], J. Jia[144], X. Jia[61], X. Jia[14a,14d], Z. Jia[14c], Y. Jiang[62a], S. Jiggins[52], J. Jimenez Pena[109], S. Jin[14c], A. Jinaru[27b], O. Jinnouchi[153], P. Johansson[138], K. A. Johns[7], D. M. Jones[32], E. Jones[166], P. Jones[32], R. W. L. Jones[90], T. J. Jones[91], R. Joshi[118], J. Jovicevic[15], X. Ju[17a], J. J. Junggeburth[36], A. Juste Rozas[13,t], S. Kabana[136e], A. Kaczmarska[85], M. Kado[74a,74b], H. Kagan[118], M. Kagan[142], A. Kahn[41], A. Kahn[127], C. Kahra[99], T. Kaji[167], E. Kajomovitz[149], N. Kakati[168], C. W. Kalderon[29], A. Kamenshchikov[154], S. Kanayama[153], N. J. Kang[135], Y. Kano[110], D. Kar[33g], K. Karava[125], M. J. Kareem[155b], E. Karentzos[54], I. Karkanias[151], S. N. Karpov[38], Z. M. Karpova[38], V. Kartvelishvili[90], A. N. Karyukhin[37], E. Kasimi[151], C. Kato[62d], J. Katzy[48], S. Kaur[34], K. Kawade[139], K. Kawagoe[88], T. Kawamoto[134], G. Kawamura[55], E. F. Kay[164], F. I. Kaya[157], S. Kazakos[13], V. F. Kazanin[37], Y. Ke[144], J. M. Keaveney[33a], R. Keeler[164], G. V. Kehris[61], J. S. Keller[34], A. S. Kelly[95], D. Kelsey[145], J. J. Kempster[20], K. E. Kennedy[41], O. Kepka[130], B. P. Kerridge[166], S. Kersten[170], B. P. Kerševan[92], S. Keshri[66], L. Keszeghova[28a], S. Ketabchi Haghighat[154], M. Khandoga[126], A. Khanov[120], A. G. Kharlamov[37], T. Kharlamova[37], E. E. Khoda[137], T. J. Khoo[18], G. Khoriauli[165], J. Khubua[148b], Y. A. R. Khwaira[66], M. Kiehn[36], A. Kilgallon[122], D. W. Kim[47a,47b], E. Kim[153], Y. K. Kim[39], N. Kimura[95], A. Kirchhoff[55], D. Kirchmeier[50], C. Kirfel[24], J. Kirk[133], A. E. Kiryunin[109], T. Kishimoto[152], D. P. Kisliuk[154], C. Kitsaki[10], O. Kivernyk[24], M. Klassen[63a], C. Klein[34], L. Klein[165], M. H. Klein[105], M. Klein[91], S. B. Klein[56], U. Klein[91], P. Klimek[36], A. Klimentov[29], F. Klimpel[109], T. Klingl[24], T. Klioutchnikova[36], F. F. Klitzner[108], P. Kluit[113], S. Kluth[109], E. Kneringer[78], T. M. Knight[154], A. Knue[54], D. Kobayashi[88], R. Kobayashi[86], M. Kocian[142], P. Kodyš[132], D. M. Koeck[145], P. T. Koenig[24], T. Koffas[34], N. M. Köhler[36], M. Kolb[134], I. Koletsou[4], T. Komarek[121], K. Köneke[54], A. X. Y. Kong[1], T. Kono[117], N. Konstantinidis[95], B. Konya[97], R. Kopeliansky[67], S. Koperny[84a], K. Korcyl[85], K. Kordas[151], G. Koren[150], A. Korn[95], S. Korn[55], I. Korolkov[13], N. Korotkova[37], B. Kortman[113], O. Kortner[109], S. Kortner[109], W. H. Kostecka[114], V. V. Kostyukhin[140], A. Kotsokechagia[134], A. Kotwal[51], A. Koulouris[36], A. Kourkoumeli-Charalampidi[72a,72b],

C. Kourkoumelis[9], E. Kourlitis[6], O. Kovanda[145], R. Kowalewski[164], W. Kozanecki[134], A. S. Kozhin[37], V. A. Kramarenko[37], G. Kramberger[92], P. Kramer[99], M. W. Krasny[126], A. Krasznahorkay[36], J. A. Kremer[99], T. Kresse[50], J. Kretzschmar[91], K. Kreul[18], P. Krieger[154], F. Krieter[108], S. Krishnamurthy[102], A. Krishnan[63b], M. Krivos[132], K. Krizka[17a], K. Kroeninger[49], H. Kroha[109], J. Kroll[130], J. Kroll[127], K. S. Krowpman[106], U. Kruchonak[38], H. Krüger[24], N. Krumnack[80], M. C. Kruse[51], J. A. Krzysiak[85], A. Kubota[153], O. Kuchinskaia[37], S. Kuday[3a], D. Kuechler[48], J. T. Kuechler[48], S. Kuehn[36], T. Kuhl[48], V. Kukhtin[38], Y. Kulchitsky[37,a], S. Kuleshov[136b,136d], M. Kumar[33g], N. Kumari[101], M. Kuna[60], A. Kupco[130], T. Kupfer[49], A. Kupich[37], O. Kuprash[54], H. Kurashige[83], L. L. Kurchaninov[155a], Y. A. Kurochkin[37], A. Kurova[37], E. S. Kuwertz[36], M. Kuze[153], A. K. Kvam[102], J. Kvita[121], T. Kwan[103], K. W. Kwok[64a], N. G. Kyriacou[105], L. A. O. Laatu[101], C. Lacasta[162], F. Lacava[74a,74b], H. Lacker[18], D. Lacour[126], N. N. Lad[95], E. Ladygin[38], B. Laforge[126], T. Lagouri[136e], S. Lai[55], I. K. Lakomiec[84a], N. Lalloue[60], J. E. Lambert[119], S. Lammers[67], W. Lampl[7], C. Lampoudis[151], A. N. Lancaster[114], E. Lançon[29], U. Landgraf[54], M. P. J. Landon[93], V. S. Lang[54], R. J. Langenberg[102], A. J. Lankford[159], F. Lanni[36], K. Lantzsch[24], A. Lanza[72a], A. Lapertosa[57a,57b], J. F. Laporte[134], T. Lari[70a], F. Lasagni Manghi[23b], M. Lassnig[36], V. Latonova[130], T. S. Lau[64a], A. Laudrain[99], A. Laurier[34], S. D. Lawlor[94], Z. Lawrence[100], M. Lazzaroni[70a,70b], B. Le[100], B. Leban[92], A. Lebedev[80], M. LeBlanc[36], T. LeCompte[6], F. Ledroit-Guillon[60], A. C. A. Lee[95], G. R. Lee[16], L. Lee[61], S. C. Lee[147], S. Lee[47a,47b], T. F. Lee[91], L. L. Leeuw[33c], H. P. Lefebvre[94], M. Lefebvre[164], C. Leggett[17a], K. Lehmann[141], G. Lehmann Miotto[36], M. Leigh[56], W. A. Leight[102], A. Leisos[151,s], M. A. L. Leite[81c], C. E. Leitgeb[48], R. Leitner[132], K. J. C. Leney[44], T. Lenz[24], S. Leone[73a], C. Leonidopoulos[52], A. Leopold[143], C. Leroy[107], R. Les[106], C. G. Lester[32], M. Levchenko[37], J. Levêque[4], D. Levin[105], L. J. Levinson[168], M. P. Lewicki[85], D. J. Lewis[20], B. Li[14b], B. Li[62b], C. Li[62a], C.-Q. Li[62c], H. Li[62a], H. Li[62b], H. Li[14c], H. Li[62b], J. Li[62c], K. Li[137], L. Li[62c], M. Li[14a,14d], Q. Y. Li[62a], S. Li[62d,62c,d], T. Li[62b], X. Li[103], Z. Li[62b], Z. Li[125], Z. Li[103], Z. Li[91], Z. Li[14a,14d], Z. Liang[14a], M. Liberatore[48], B. Liberti[75a], K. Lie[64c], J. Lieber Marin[81b], K. Lin[106], R. A. Linck[67], R. E. Lindley[7], J. H. Lindon[2], A. Linss[48], E. Lipeles[127], A. Lipniacka[16], A. Lister[163], J. D. Little[4], B. Liu[14a], B. X. Liu[141], D. Liu[62d,62c], J. B. Liu[62a], J. K. K. Liu[32], K. Liu[62d,62c], M. Liu[62a], M. Y. Liu[62a], P. Liu[14a], Q. Liu[62c,62d,137], X. Liu[62a], Y. Liu[48], Y. Liu[14c,14d], Y. L. Liu[105], Y. W. Liu[62a], M. Livan[72a,72b], J. Llorente Merino[141], S. L. Lloyd[93], E. M. Lobodzinska[48], P. Loch[7], S. Loffredo[75a,75b], T. Lohse[18], K. Lohwasser[138], M. Lokajicek[130], J. D. Long[161], I. Longarini[74a,74b], L. Longo[69a,69b], R. Longo[161], I. Lopez Paz[36], A. Lopez Solis[48], J. Lorenz[108], N. Lorenzo Martinez[4], A. M. Lory[108], A. Lösle[54], X. Lou[47a,47b], X. Lou[14a,14d], A. Lounis[66], J. Love[6], P. A. Love[90], J. J. Lozano Bahilo[162], G. Lu[14a,14d], M. Lu[79], S. Lu[127], Y. J. Lu[65], H. J. Lubatti[137], C. Luci[74a,74b], F. L. Lucio Alves[14c], A. Lucotte[60], F. Luehring[67], I. Luise[144], O. Lukianchuk[66], O. Lundberg[143], B. Lund-Jensen[143], N. A. Luongo[122], M. S. Lutz[150], D. Lynn[29], H. Lyons[91], R. Lysak[130], E. Lytken[97], F. Lyu[14a], V. Lyubushkin[38], T. Lyubushkina[38], H. Ma[29], L. L. Ma[62b], Y. Ma[95], D. M. Mac Donell[164], G. Maccarrone[53], J. C. MacDonald[138], R. Madar[40], W. F. Mader[50], J. Maeda[83], T. Maeno[29], M. Maerker[50], V. Magerl[54], J. Magro[68a,68c], H. Maguire[138], D. J. Mahon[41], C. Maidantchik[81b], A. Maio[129a,129b,129d], K. Maj[84a], O. Majersky[28a], S. Majewski[122], N. Makovec[66], V. Maksimovic[15], B. Malaescu[126], Pa. Malecki[85], V. P. Maleev[37], F. Malek[60], D. Malito[43a,43b], U. Mallik[79], C. Malone[32], S. Maltezos[10], S. Malyukov[38], J. Mamuzic[13], G. Mancini[53], G. Manco[72a,72b], J. P. Mandalia[93], I. Mandić[92], L. Manhaes de Andrade Filho[81a], I. M. Maniatis[151], M. Manisha[134], J. Manjarres Ramos[50], D. C. Mankad[168], A. Mann[108], B. Mansoulie[134], S. Manzoni[36], A. Marantis[151], G. Marchiori[5], M. Marcisovsky[130], L. Marcoccia[75a,75b], C. Marcon[70a,70b], M. Marinescu[20], M. Marjanovic[119], Z. Marshall[17a], S. Marti-Garcia[162], T. A. Martin[166], V. J. Martin[52], B. Martin dit Latour[16], L. Martinelli[74a,74b], M. Martinez[13,t], P. Martinez Agullo[162], V. I. Martinez Outschoorn[102], P. Martinez Suarez[13], S. Martin-Haugh[133], V. S. Martoiu[27b], A. C. Martyniuk[95], A. Marzin[36], S. R. Maschek[109], L. Masetti[99], T. Mashimo[152], J. Masik[100], A. L. Maslennikov[37], L. Massa[23b], P. Massarotti[71a,71b], P. Mastrandrea[73a,73b], A. Mastroberardino[43a,43b], T. Masubuchi[152], T. Mathisen[160], N. Matsuzawa[152], J. Maurer[27b], B. Maček[92], D. A. Maximov[37], R. Mazini[147], I. Maznas[151], M. Mazza[106], S. M. Mazza[135], C. Mc Ginn[29,ad], J. P. Mc Gowan[103], S. P. Mc Kee[105], T. G. McCarthy[109], W. P. McCormack[17a], E. F. McDonald[104], A. E. McDougall[113], J. A. Mcfayden[145], G. Mchedlidze[148b], R. P. Mckenzie[33g], T. C. Mclachlan[48], D. J. Mclaughlin[95], K. D. McLean[164], S. J. McMahon[133], P. C. McNamara[104], C. M. Mcpartland[91], R. A. McPherson[164,v], T. Megy[40], S. Mehlhase[108], A. Mehta[91], B. Meirose[45], D. Melini[149], B. R. Mellado Garcia[33g], A. H. Melo[55],

F. Meloni[48], E. D. Mendes Gouveia[129a], A. M. Mendes Jacques Da Costa[20], H. Y. Meng[154], L. Meng[90], S. Menke[109], M. Mentink[36], E. Meoni[43a,43b], C. Merlassino[125], L. Merola[71a,71b], C. Meroni[70a], G. Merz[105], O. Meshkov[37], J. K. R. Meshreki[140], J. Metcalfe[6], A. S. Mete[6], C. Meyer[67], J.-P. Meyer[134], M. Michetti[18], R. P. Middleton[133], L. Mijović[52], G. Mikenberg[168], M. Mikestikova[130], M. Mikuž[92], H. Mildner[138], A. Milic[154], C. D. Milke[44], D. W. Miller[39], L. S. Miller[34], A. Milov[168], D. A. Milstead[47a,47b], T. Min[14c], A. A. Minaenko[37], I. A. Minashvili[148b], L. Mince[59], A. I. Mincer[116], B. Mindur[84a], M. Mineev[38], Y. Mino[86], L. M. Mir[13], M. Miralles Lopez[162], M. Mironova[125], T. Mitani[167], A. Mitra[166], V. A. Mitsou[162], O. Miu[154], P. S. Miyagawa[93], Y. Miyazaki[88], A. Mizukami[82], J. U. Mjörnmark[97], T. Mkrtchyan[63a], T. Mlinarevic[95], M. Mlynarikova[36], T. Moa[47a,47b], S. Mobius[55], K. Mochizuki[107], P. Moder[48], P. Mogg[108], A. F. Mohammed[14a,14d], S. Mohapatra[41], G. Mokgatitswane[33g], B. Mondal[140], S. Mondal[131], K. Mönig[48], E. Monnier[101], L. Monsonis Romero[162], J. Montejo Berlingen[36], M. Montella[118], F. Monticelli[89], N. Morange[66], A. L. Moreira De Carvalho[129a], M. Moreno Llácer[162], C. Moreno Martinez[13], P. Morettini[57b], S. Morgenstern[166], M. Morii[61], M. Morinaga[152], V. Morisbak[124], A. K. Morley[36], F. Morodei[74a,74b], L. Morvaj[36], P. Moschovakos[36], B. Moser[36], M. Mosidze[148b], T. Moskalets[54], P. Moskvitina[112], J. Moss[31,n], E. J. W. Moyse[102], S. Muanza[101], J. Mueller[128], D. Muenstermann[90], R. Müller[19], G. A. Mullier[97], J. J. Mullin[127], D. P. Mungo[70a,70b], J. L. Munoz Martinez[13], D. Munoz Perez[162], F. J. Munoz Sanchez[100], M. Murin[100], W. J. Murray[133,166], A. Murrone[70a,70b], J. M. Muse[119], M. Muškinja[17a], C. Mwewa[29], A. G. Myagkov[37,a], A. J. Myers[8], A. A. Myers[128], G. Myers[67], M. Myska[131], B. P. Nachman[17a], O. Nackenhorst[49], A. Nag[50], K. Nagai[125], K. Nagano[82], J. L. Nagle[29,ad], E. Nagy[101], A. M. Nairz[36], Y. Nakahama[82], K. Nakamura[82], H. Nanjo[123], R. Narayan[44], E. A. Narayanan[111], I. Naryshkin[37], M. Naseri[34], C. Nass[24], G. Navarro[22a], J. Navarro-Gonzalez[162], R. Nayak[150], A. Nayaz[18], P. Y. Nechaeva[37], F. Nechansky[48], L. Nedic[125], T. J. Neep[20], A. Negri[72a,72b], M. Negrini[23b], C. Nellist[112], C. Nelson[103], K. Nelson[105], S. Nemecek[130], M. Nessi[36,g], M. S. Neubauer[161], F. Neuhaus[99], J. Neundorf[48], R. Newhouse[163], P. R. Newman[20], C. W. Ng[128], Y. S. Ng[18], Y. W. Y. Ng[159], B. Ngair[35e], H. D. N. Nguyen[107], R. B. Nickerson[125], R. Nicolaidou[134], J. Nielsen[135], M. Niemeyer[55], N. Nikiforou[36], V. Nikolaenko[37,a], I. Nikolic-Audit[126], K. Nikolopoulos[20], P. Nilsson[29], H. R. Nindhito[56], A. Nisati[74a], N. Nishu[2], R. Nisius[109], J.-E. Nitschke[50], E. K. Nkadimeng[33g], S. J. Noacco Rosende[89], T. Nobe[152], D. L. Noel[32], Y. Noguchi[86], T. Nommensen[146], M. A. Nomura[29], M. B. Norfolk[138], R. R. B. Norisam[95], B. J. Norman[34], J. Novak[92], T. Novak[48], O. Novgorodova[50], L. Novotny[131], R. Novotny[111], L. Nozka[121], K. Ntekas[159], E. Nurse[95], F. G. Oakham[34,aa], J. Ocariz[126], A. Ochi[83], I. Ochoa[129a], S. Oerdek[160], A. Ogrodnik[84a], A. Oh[100], C. C. Ohm[143], H. Oide[153], R. Oishi[152], M. L. Ojeda[48], Y. Okazaki[86], M. W. O'Keefe[91], Y. Okumura[152], A. Olariu[27b], L. F. Oleiro Seabra[129a], S. A. Olivares Pino[136e], D. Oliveira Damazio[29], D. Oliveira Goncalves[81a], J. L. Oliver[159], M. J. R. Olsson[159], A. Olszewski[85], J. Olszowska[85,*], Ö.O. Öncel[54], D. C. O'Neil[141], A. P. O'Neill[19], A. Onofre[129a,129e], P. U. E. Onyisi[11], M. J. Oreglia[39], G. E. Orellana[89], D. Orestano[76a,76b], N. Orlando[13], R. S. Orr[154], V. O'Shea[59], R. Ospanov[62a], G. Otero y Garzon[30], H. Otono[88], P. S. Ott[63a], G. J. Ottino[17a], M. Ouchrif[35d], J. Ouellette[29,ad], F. Ould-Saada[124], M. Owen[59], R. E. Owen[133], K. Y. Oyulmaz[21a], V. E. Ozcan[21a], N. Ozturk[8], S. Ozturk[21d], J. Pacalt[121], H. A. Pacey[32], K. Pachal[51], A. Pacheco Pages[13], C. Padilla Aranda[13], G. Padovano[74a,74b], S. Pagan Griso[17a], G. Palacino[67], A. Palazzo[69a,69b], S. Palazzo[52], S. Palestini[36], M. Palka[84b], J. Pan[171], T. Pan[64a], D. K. Panchal[11], C. E. Pandini[113], J. G. Panduro Vazquez[94], H. Pang[14b], P. Pani[48], G. Panizzo[68a,68c], L. Paolozzi[56], C. Papadatos[107], S. Parajuli[44], A. Paramonov[6], C. Paraskevopoulos[10], D. Paredes Hernandez[64b], T. H. Park[154], M. A. Parker[32], F. Parodi[57a,57b], E. W. Parrish[114], V. A. Parrish[52], J. A. Parsons[41], U. Parzefall[54], B. Pascual Dias[107], L. Pascual Dominguez[150], V. R. Pascuzzi[17a], F. Pasquali[113], E. Pasqualucci[74a], S. Passaggio[57b], F. Pastore[94], P. Pasuwan[47a,47b], P. Patel[85], J. R. Pater[100], J. Patton[91], T. Pauly[36], J. Pearkes[142], M. Pedersen[124], R. Pedro[129a], S. V. Peleganchuk[37], O. Penc[36], E. A. Pender[52], C. Peng[64b], H. Peng[62a], K. E. Penski[108], M. Penzin[37], B. S. Peralva[81d], A. P. Pereira Peixoto[60], L. Pereira Sanchez[47a,47b], D. V. Perepelitsa[29,ad], E. Perez Codina[155a], M. Perganti[10], L. Perini[70a,70b,*], H. Pernegger[36], S. Perrella[36], A. Perrevoort[112], O. Perrin[40], K. Peters[48], R. F. Y. Peters[100], B. A. Petersen[36], T. C. Petersen[42], E. Petit[101], V. Petousis[131], C. Petridou[151], A. Petrukhin[140], M. Pettee[17a], N. E. Pettersson[36], A. Petukhov[37], K. Petukhova[132], A. Peyaud[134], R. Pezoa[136f], L. Pezzotti[36], G. Pezzullo[171], T. M. Pham[169], T. Pham[104], P. W. Phillips[133], M. W. Phipps[161], G. Piacquadio[144], E. Pianori[17a], F. Piazza[70a,70b], R. Piegaia[30], D. Pietreanu[27b], A. D. Pilkington[100], M. Pinamonti[68a,68c], J. L. Pinfold[2], B. C. Pinheiro Pereira[129a], C. Pitman Donaldson[95], D. A. Pizzi[34], L. Pizzimento[75a,75b],

A. Pizzini[113], M. -A. Pleier[29], V. Plesanovs[54], V. Pleskot[132], E. Plotnikova[38], G. Poddar[4], R. Poettgen[97], L. Poggioli[126], I. Pogrebnyak[106], D. Pohl[24], I. Pokharel[55], S. Polacek[132], G. Polesello[72a], A. Poley[141,155a], R. Polifka[131], A. Polini[23b], C. S. Pollard[125], Z. B. Pollock[118], V. Polychronakos[29], E. Pompa Pacchi[74a,74b], D. Ponomarenko[37], L. Pontecorvo[36], S. Popa[27a], G. A. Popeneciu[27d], D. M. Portillo Quintero[155a], S. Pospisil[131], P. Postolache[27c], K. Potamianos[125], I. N. Potrap[38], C. J. Potter[32], H. Potti[1], T. Poulsen[48], J. Poveda[162], M. E. Pozo Astigarraga[36], A. Prades Ibanez[162], M. M. Prapa[46], J. Pretel[54], D. Price[100], M. Primavera[69a], M. A. Principe Martin[98], M. L. Proffitt[137], N. Proklova[127], K. Prokofiev[64c], G. Proto[75a,75b], S. Protopopescu[29], J. Proudfoot[6], M. Przybycien[84a], J. E. Puddefoot[138], D. Pudzha[37], P. Puzo[66], D. Pyatiizbyantseva[37], J. Qian[105], D. Qichen[100], Y. Qin[100], T. Qiu[93], A. Quadt[55], M. Queitsch-Maitland[100], G. Quetant[56], G. Rabanal Bolanos[61], D. Rafanoharana[54], F. Ragusa[70a,70b], J. L. Rainbolt[39], J. A. Raine[56], S. Rajagopalan[29], E. Ramakoti[37], K. Ran[14d,48], V. Raskina[126], D. F. Rassloff[63a], S. Rave[99], B. Ravina[55], I. Ravinovich[168], M. Raymond[36], A. L. Read[124], N. P. Readioff[138], D. M. Rebuzzi[72a,72b], G. Redlinger[29], K. Reeves[45], J. A. Reidelsturz[170], D. Reikher[150], A. Reiss[99], A. Rej[140], C. Rembser[36], A. Renardi[48], M. Renda[27b], M. B. Rendel[109], A. G. Rennie[59], S. Resconi[70a], M. Ressegotti[57a,57b], E. D. Resseguie[17a], S. Rettie[95], B. Reynolds[118], E. Reynolds[17a], M. Rezaei Estabragh[170], O. L. Rezanova[37], P. Reznicek[132], E. Ricci[77a,77b], R. Richter[109], S. Richter[47a,47b], E. Richter-Was[84b], M. Ridel[126], P. Rieck[116], P. Riedler[36], M. Rijssenbeek[144], A. Rimoldi[72a,72b], M. Rimoldi[48], L. Rinaldi[23a,23b], T. T. Rinn[29], M. P. Rinnagel[108], G. Ripellino[143], I. Riu[13], P. Rivadeneira[48], J. C. Rivera Vergara[164], F. Rizatdinova[120], E. Rizvi[93], C. Rizzi[56], B. A. Roberts[166], B. R. Roberts[17a], S. H. Robertson[103,v], M. Robin[48], D. Robinson[32], C. M. Robles Gajardo[136f], M. Robles Manzano[99], A. Robson[59], A. Rocchi[75a,75b], C. Roda[73a,73b], S. Rodriguez Bosca[63a], Y. Rodriguez Garcia[22a], A. Rodriguez Rodriguez[54], A. M. Rodríguez Vera[155b], S. Roe[36], J. T. Roemer[159], A. R. Roepe-Gier[119], J. Roggel[170], O. Røhne[124], R. A. Rojas[164], B. Roland[54], C. P. A. Roland[67], J. Roloff[29], A. Romaniouk[37], E. Romano[72a,72b], M. Romano[23b], A. C. Romero Hernandez[161], N. Rompotis[91], L. Roos[126], S. Rosati[74a], B. J. Rosser[39], E. Rossi[4], E. Rossi[71a,71b], L. P. Rossi[57b], L. Rossini[48], R. Rosten[118], M. Rotaru[27b], B. Rottler[54], D. Rousseau[66], D. Rousso[32], G. Rovelli[72a,72b], A. Roy[161], A. Rozanov[101], Y. Rozen[149], X. Ruan[33g], A. Rubio Jimenez[162], A. J. Ruby[91], V. H. Ruelas Rivera[18], T. A. Ruggeri[1], F. Rühr[54], A. Ruiz-Martinez[162], A. Rummler[36], Z. Rurikova[54], N. A. Rusakovich[38], H. L. Russell[164], J. P. Rutherfoord[7], K. Rybacki[90], M. Rybar[132], E. B. Rye[124], A. Ryzhov[37], J. A. Sabater Iglesias[56], P. Sabatini[162], L. Sabetta[74a,74b], H.F.-W. Sadrozinski[135], F. Safai Tehrani[74a], B. Safarzadeh Samani[145], M. Safdari[142], S. Saha[103], M. Sahinsoy[109], M. Saimpert[134], M. Saito[152], T. Saito[152], D. Salamani[36], G. Salamanna[76a,76b], A. Salnikov[142], J. Salt[162], A. Salvador Salas[13], D. Salvatore[43a,43b], F. Salvatore[145], A. Salzburger[36], D. Sammel[54], D. Sampsonidis[151], D. Sampsonidou[62d,62c], J. Sánchez[162], A. Sanchez Pineda[4], V. Sanchez Sebastian[162], H. Sandaker[124], C. O. Sander[48], J. A. Sandesara[102], M. Sandhoff[170], C. Sandoval[22b], D. P. C. Sankey[133], A. Sansoni[53], L. Santi[74a,74b], C. Santoni[40], H. Santos[129a,129b], S. N. Santpur[17a], A. Santra[168], K. A. Saoucha[138], J. G. Saraiva[129a,129d], J. Sardain[7], O. Sasaki[82], K. Sato[156], C. Sauer[63b], F. Sauerburger[54], E. Sauvan[4], P. Savard[154,aa], R. Sawada[152], C. Sawyer[133], L. Sawyer[96], I. Sayago Galvan[162], C. Sbarra[23b], A. Sbrizzi[23a,23b], T. Scanlon[95], J. Schaarschmidt[137], P. Schacht[109], D. Schaefer[39], U. Schäfer[99], A. C. Schaffer[66], D. Schaile[108], R. D. Schamberger[144], E. Schanet[108], C. Scharf[18], V. A. Schegelsky[37], D. Scheirich[132], F. Schenck[18], M. Schernau[159], C. Scheulen[55], C. Schiavi[57a,57b], Z. M. Schillaci[26], E. J. Schioppa[69a,69b], M. Schioppa[43a,43b], B. Schlag[99], K. E. Schleicher[54], S. Schlenker[36], K. Schmieden[99], C. Schmitt[99], S. Schmitt[48], L. Schoeffel[134], A. Schoening[63b], P. G. Scholer[54], E. Schopf[125], M. Schott[99], J. Schovancova[36], S. Schramm[56], F. Schroeder[170], H.-C. Schultz-Coulon[63a], M. Schumacher[54], B. A. Schumm[135], Ph. Schune[134], A. Schwartzman[142], T. A. Schwarz[105], Ph. Schwemling[134], R. Schwienhorst[106], A. Sciandra[135], G. Sciolla[26], F. Scuri[73a], F. Scutti[104], C. D. Sebastiani[91], K. Sedlaczek[49], P. Seema[18], S. C. Seidel[111], A. Seiden[135], B. D. Seidlitz[41], T. Seiss[39], C. Seitz[48], J. M. Seixas[81b], G. Sekhniaidze[71a], S. J. Sekula[44], L. Selem[4], N. Semprini-Cesari[23a,23b], S. Sen[51], D. Sengupta[56], V. Senthilkumar[162], L. Serin[66], L. Serkin[68a,68b], M. Sessa[76a,76b], H. Severini[119], S. Sevova[142], F. Sforza[57a,57b], A. Sfyrla[56], E. Shabalina[55], R. Shaheen[143], J. D. Shahinian[127], N. W. Shaikh[47a,47b], D. Shaked Renous[168], L. Y. Shan[14a], M. Shapiro[17a], A. Sharma[36], A. S. Sharma[163], P. Sharma[79], S. Sharma[48], P. B. Shatalov[37], K. Shaw[145], S. M. Shaw[100], Q. Shen[5,62c], P. Sherwood[95], L. Shi[95], C. O. Shimmin[171], Y. Shimogama[167], J. D. Shinner[94], I. P. J. Shipsey[125], S. Shirabe[60], M. Shiyakova[38], J. Shlomi[168], M. J. Shochet[39], J. Shojaii[104], D. R. Shope[124], S. Shrestha[118,ae], E. M. Shrif[33g], M. J. Shroff[164], P. Sicho[130], A. M. Sickles[161], E. Sideras Haddad[33g],

A. Sidoti[23b], F. Siegert[50], Dj. Sijacki[15], R. Sikora[84a], F. Sili[89], J. M. Silva[20], M. V. Silva Oliveira[36], S. B. Silverstein[47a], S. Simion[66], R. Simoniello[36], E. L. Simpson[59], N. D. Simpson[97], S. Simsek[21d], S. Sindhu[55], P. Sinervo[154], V. Sinetckii[37], S. Singh[141], S. Singh[154], S. Sinha[48], S. Sinha[33g], M. Sioli[23a,23b], I. Siral[122], S. Yu. Sivoklokov[37,*], J. Sjölin[47a,47b], A. Skaf[55], E. Skorda[97], P. Skubic[119], M. Slawinska[85], V. Smakhtin[168], B. H. Smart[133], J. Smiesko[36], S. Yu. Smirnov[37], Y. Smirnov[37], L. N. Smirnova[37,a], O. Smirnova[97], A. C. Smith[41], E. A. Smith[39], H. A. Smith[125], J. L. Smith[91], R. Smith[142], M. Smizanska[90], K. Smolek[131], A. Smykiewicz[85], A. A. Snesarev[37], H. L. Snoek[113], S. Snyder[29], R. Sobie[164,v], A. Soffer[150], C. A. Solans Sanchez[36], E. Yu. Soldatov[37], U. Soldevila[162], A. A. Solodkov[37], S. Solomon[54], A. Soloshenko[38], K. Solovieva[54], O. V. Solovyanov[37], V. Solovyev[37], P. Sommer[36], A. Sonay[13], W. Y. Song[155b], A. Sopczak[131], A. L. Sopio[95], F. Sopkova[28b], V. Sothilingam[63a], S. Sottocornola[72a,72b], R. Soualah[115b], Z. Soumaimi[35e], D. South[48], S. Spagnolo[69a,69b], M. Spalla[109], F. Spanò[94], D. Sperlich[54], G. Spigo[36], M. Spina[145], S. Spinali[90], D. P. Spiteri[59], M. Spousta[132], E. J. Staats[34], A. Stabile[70a,70b], R. Stamen[63a], M. Stamenkovic[113], A. Stampekis[20], M. Standke[24], E. Stanecka[85], M. V. Stange[50], B. Stanislaus[17a], M. M. Stanitzki[48], M. Stankaityte[125], B. Stapf[48], E. A. Starchenko[37], G. H. Stark[135], J. Stark[101], D. M. Starko[155b], P. Staroba[130], P. Starovoitov[63a], S. Stärz[103], R. Staszewski[85], G. Stavropoulos[46], J. Steentoft[160], P. Steinberg[29], A. L. Steinhebel[122], B. Stelzer[141,155a], H. J. Stelzer[128], O. Stelzer-Chilton[155a], H. Stenzel[58], T. J. Stevenson[145], G. A. Stewart[36], M. C. Stockton[36], G. Stoicea[27b], M. Stolarski[129a], S. Stonjek[109], A. Straessner[50], J. Strandberg[143], S. Strandberg[47a,47b], M. Strauss[119], T. Strebler[101], P. Strizenec[28b], R. Ströhmer[165], D. M. Strom[122], L. R. Strom[48], R. Stroynowski[44], A. Strubig[47a,47b], S. A. Stucci[29], B. Stugu[16], J. Stupak[119], N. A. Styles[48], D. Su[142], S. Su[62a], W. Su[62c,62d,137], X. Su[62a,66], K. Sugizaki[152], V. V. Sulin[37], M. J. Sullivan[91], D. M. S. Sultan[77a,77b], L. Sultanaliyeva[37], S. Sultansoy[3b], T. Sumida[86], S. Sun[105], S. Sun[169], O. Sunneborn Gudnadottir[160], M. R. Sutton[145], M. Svatos[130], M. Swiatlowski[155a], T. Swirski[165], I. Sykora[28a], M. Sykora[132], T. Sykora[132], D. Ta[99], K. Tackmann[48,u], A. Taffard[159], R. Tafirout[155a], J. S. Tafoya Vargas[66], R. H. M. Taibah[126], R. Takashima[87], K. Takeda[83], E. P. Takeva[52], Y. Takubo[82], M. Talby[101], A. A. Talyshev[37], K. C. Tam[64b], N. M. Tamir[150], A. Tanaka[152], J. Tanaka[152], R. Tanaka[66], M. Tanasini[57a,57b], J. Tang[62c], Z. Tao[163], S. Tapia Araya[80], S. Tapprogge[99], A. Tarek Abouelfadl Mohamed[106], S. Tarem[149], K. Tariq[62b], G. Tarna[27b], G. F. Tartarelli[70a], P. Tas[132], M. Tasevsky[130], E. Tassi[43a,43b], A. C. Tate[161], G. Tateno[152], Y. Tayalati[35e], G. N. Taylor[104], W. Taylor[155b], H. Teagle[91], A. S. Tee[169], R. Teixeira De Lima[142], P. Teixeira-Dias[94], J. J. Teoh[154], K. Terashi[152], J. Terron[98], S. Terzo[13], M. Testa[53], R. J. Teuscher[154,v], A. Thaler[78], O. Theiner[56], N. Themistokleous[52], T. Theveneaux-Pelzer[18], O. Thielmann[170], D. W. Thomas[94], J. P. Thomas[20], E. A. Thompson[48], P. D. Thompson[20], E. Thomson[127], E. J. Thorpe[93], Y. Tian[55], V. Tikhomirov[37,a], Yu. A. Tikhonov[37], S. Timoshenko[37], E. X. L. Ting[1], P. Tipton[171], S. Tisserant[101], S. H. Tlou[33g], A. Tnourji[40], K. Todome[23a,23b], S. Todorova-Nova[132], S. Todt[50], M. Togawa[82], J. Tojo[88], S. Tokár[28a], K. Tokushuku[82], R. Tombs[32], M. Tomoto[82,110], L. Tompkins[142], K. W. Topolnicki[84b], P. Tornambe[102], E. Torrence[122], H. Torres[50], E. Torró Pastor[162], M. Toscani[30], C. Tosciri[39], D. R. Tovey[138], A. Traeet[16], I. S. Trandafir[27b], T. Trefzger[165], A. Tricoli[29], I. M. Trigger[155a], S. Trincaz-Duvoid[126], D. A. Trischuk[26], B. Trocmé[60], A. Trofymov[66], C. Troncon[70a], L. Truong[33c], M. Trzebinski[85], A. Trzupek[85], F. Tsai[144], M. Tsai[105], A. Tsiamis[151], P. V. Tsiareshka[37], S. Tsigaridas[155a], A. Tsirigotis[151,s], V. Tsiskaridze[144], E. G. Tskhadadze[148a], M. Tsopoulou[151], Y. Tsujikawa[86], I. I. Tsukerman[37], V. Tsulaia[17a], S. Tsuno[82], O. Tsur[149], D. Tsybychev[144], Y. Tu[64b], A. Tudorache[27b], V. Tudorache[27b], A. N. Tuna[36], S. Turchikhin[38], I. Turk Cakir[3a], R. Turra[70a], T. Turtuvshin[38], P. M. Tuts[41], S. Tzamarias[151], P. Tzanis[10], E. Tzovara[99], K. Uchida[152], F. Ukegawa[156], P. A. Ulloa Poblete[136c], G. Unal[36], M. Unal[11], A. Undrus[29], G. Unel[159], J. Urban[28b], P. Urquijo[104], G. Usai[8], R. Ushioda[153], M. Usman[107], Z. Uysal[21b], V. Vacek[131], B. Vachon[103], K. O. H. Vadla[124], T. Vafeiadis[36], C. Valderanis[108], E. Valdes Santurio[47a,47b], M. Valente[155a], S. Valentinetti[23a,23b], A. Valero[162], A. Vallier[101], J. A. Valls Ferrer[162], T. R. Van Daalen[137], P. Van Gemmeren[6], M. Van Rijnbach[36,124], S. Van Stroud[95], I. Van Vulpen[113], M. Vanadia[75a,75b], W. Vandelli[36], M. Vandenbroucke[134], E. R. Vandewall[120], D. Vannicola[150], L. Vannoli[57a,57b], R. Vari[74a], E. W. Varnes[7], C. Varni[17a], T. Varol[147], D. Varouchas[66], L. Varriale[162], K. E. Varvell[146], M. E. Vasile[27b], L. Vaslin[40], G. A. Vasquez[164], F. Vazeille[40], T. Vazquez Schroeder[36], J. Veatch[31], V. Vecchio[100], M. J. Veen[102], I. Veliscek[125], L. M. Veloce[154], F. Veloso[129a,129c], S. Veneziano[74a], A. Ventura[69a,69b], A. Verbytskyi[109], M. Verducci[73a,73b], C. Vergis[24], M. Verissimo De Araujo[81b], W. Verkerke[113], J. C. Vermeulen[113], C. Vernieri[142], P. J. Verschuuren[94], M. Vessella[102], M. C. Vetterli[141,aa],

A. Vgenopoulos[151], N. Viaux Maira[136f], T. Vickey[138], O. E. Vickey Boeriu[138], G. H. A. Viehhauser[125], L. Vigani[63b], M. Villa[23a,23b], M. Villaplana Perez[162], E. M. Villhauer[52], E. Vilucchi[53], M. G. Vincter[34], G. S. Virdee[20], A. Vishwakarma[52], C. Vittori[23a,23b], I. Vivarelli[145], V. Vladimirov[166], E. Voevodina[109], F. Vogel[108], P. Vokac[131], J. Von Ahnen[48], E. Von Toerne[24], B. Vormwald[36], V. Vorobel[132], K. Vorobev[37], M. Vos[162], J. H. Vossebeld[91], M. Vozak[113], L. Vozdecky[93], N. Vranjes[15], M. Vranjes Milosavljevic[15], M. Vreeswijk[113], R. Vuillermet[36], O. Vujinovic[99], I. Vukotic[39], S. Wada[156], C. Wagner[102], W. Wagner[170], S. Wahdan[170], H. Wahlberg[89], R. Wakasa[156], M. Wakida[110], V. M. Walbrecht[109], J. Walder[133], R. Walker[108], W. Walkowiak[140], A. M. Wang[61], A. Z. Wang[169], C. Wang[62a], C. Wang[62c], H. Wang[17a], J. Wang[64a], P. Wang[44], R. -J. Wang[99], R. Wang[61], R. Wang[6], S. M. Wang[147], S. Wang[62b], T. Wang[62a], W. T. Wang[79], W. X. Wang[62a], X. Wang[14c], X. Wang[161], X. Wang[62c], Y. Wang[62d], Y. Wang[14c], Z. Wang[105], Z. Wang[51,62c,62d], Z. Wang[105], A. Warburton[103], R. J. Ward[20], N. Warrack[59], A. T. Watson[20], M. F. Watson[20], G. Watts[137], B. M. Waugh[95], A. F. Webb[11], C. Weber[29], M. S. Weber[19], S. M. Weber[63a], C. Wei[62a], Y. Wei[125], A. R. Weidberg[125], J. Weingarten[49], M. Weirich[99], C. Weiser[54], C. J. Wells[48], T. Wenaus[29], B. Wendland[49], T. Wengler[36], N. S. Wenke[109], N. Wermes[24], M. Wessels[63a], K. Whalen[122], A. M. Wharton[90], A. S. White[61], A. White[8], M. J. White[1], D. Whiteson[159], L. Wickremasinghe[123], W. Wiedenmann[169], C. Wiel[50], M. Wielers[133], N. Wieseotte[99], C. Wiglesworth[42], L. A. M. Wiik-Fuchs[54], D. J. Wilbern[119], H. G. Wilkens[36], D. M. Williams[41], H. H. Williams[127], S. Williams[32], S. Willocq[102], P. J. Windischhofer[125], F. Winklmeier[122], B. T. Winter[54], M. Wittgen[142], M. Wobisch[96], R. Wölker[125], J. Wollrath[159], M. W. Wolter[85], H. Wolters[129a,129c], V. W. S. Wong[163], A. F. Wongel[48], S. D. Worm[48], B. K. Wosiek[85], K. W. Woźniak[85], K. Wraight[59], J. Wu[14a,14d], M. Wu[64a], M. Wu[112], S. L. Wu[169], X. Wu[56], Y. Wu[62a], Z. Wu[134,62a], J. Wuerzinger[125], T. R. Wyatt[100], B. M. Wynne[52], S. Xella[42], L. Xia[14c], M. Xia[14b], J. Xiang[64c], X. Xiao[105], M. Xie[62a], X. Xie[62a], J. Xiong[17a], I. Xiotidis[145], D. Xu[14a], H. Xu[62a], H. Xu[62a], L. Xu[62a], R. Xu[127], T. Xu[105], W. Xu[105], Y. Xu[14b], Z. Xu[62b], Z. Xu[142], B. Yabsley[146], S. Yacoob[33a], N. Yamaguchi[88], Y. Yamaguchi[153], H. Yamauchi[156], T. Yamazaki[17a], Y. Yamazaki[83], J. Yan[62c], S. Yan[125], Z. Yan[25], H. J. Yang[62c,62d], H. T. Yang[17a], S. Yang[62a], T. Yang[64c], X. Yang[62a], X. Yang[14a], Y. Yang[44], Z. Yang[62a,105], W.-M. Yao[17a], Y. C. Yap[48], H. Ye[14c], J. Ye[44], S. Ye[29], X. Ye[62a], Y. Yeh[95], I. Yeletskikh[38], M. R. Yexley[90], P. Yin[41], K. Yorita[167], C. J. S. Young[54], C. Young[142], M. Yuan[105], R. Yuan[62b,j], L. Yue[95], X. Yue[63a], M. Zaazoua[35e], B. Zabinski[85], E. Zaid[52], T. Zakareishvili[148b], N. Zakharchuk[34], S. Zambito[56], J. A. Zamora Saa[136d], J. Zang[152], D. Zanzi[54], O. Zaplatilek[131], S. V. Zeißner[49], C. Zeitnitz[170], J. C. Zeng[161], D. T. Zenger Jr[26], O. Zenin[37], T. Ženiš[28a], S. Zenz[93], S. Zerradi[35a], D. Zerwas[66], B. Zhang[14c], D. F. Zhang[138], G. Zhang[14b], J. Zhang[62b], J. Zhang[6], K. Zhang[14a,14d], L. Zhang[14c], P. Zhang[14a,14d], R. Zhang[169], S. Zhang[105], T. Zhang[152], X. Zhang[62c], X. Zhang[62b], Z. Zhang[17a], Z. Zhang[66], H. Zhao[137], P. Zhao[51], T. Zhao[62b], Y. Zhao[135], Z. Zhao[62a], A. Zhemchugov[38], X. Zheng[62a], Z. Zheng[142], D. Zhong[161], B. Zhou[105], C. Zhou[169], H. Zhou[7], N. Zhou[62c], Y. Zhou[7], C. G. Zhu[62b], C. Zhu[14a,14d], H. L. Zhu[62a], H. Zhu[14a], J. Zhu[105], Y. Zhu[62c], Y. Zhu[62a], X. Zhuang[14a], K. Zhukov[37], V. Zhulanov[37], N. I. Zimine[38], J. Zinsser[63b], M. Ziolkowski[140], L. Živković[15], A. Zoccoli[23a,23b], K. Zoch[56], T. G. Zorbas[138], O. Zormpa[46], W. Zou[41], L. Zwalinski[36]

[1] Department of Physics, University of Adelaide, Adelaide, Australia
[2] Department of Physics, University of Alberta, Edmonton, AB, Canada
[3] [(a)]Department of Physics, Ankara University, Ankara, Türkiye; [(b)]Division of Physics, TOBB University of Economics and Technology, Ankara, Türkiye
[4] LAPP, Univ. Savoie Mont Blanc, CNRS/IN2P3, Annecy, France
[5] APC, Université Paris Cité, CNRS/IN2P3, Paris, France
[6] High Energy Physics Division, Argonne National Laboratory, Argonne, IL, USA
[7] Department of Physics, University of Arizona, Tucson, AZ, USA
[8] Department of Physics, University of Texas at Arlington, Arlington, TX, USA
[9] Physics Department, National and Kapodistrian University of Athens, Athens, Greece
[10] Physics Department, National Technical University of Athens, Zografou, Greece
[11] Department of Physics, University of Texas at Austin, Austin, TX, USA
[12] Institute of Physics, Azerbaijan Academy of Sciences, Baku, Azerbaijan
[13] Institut de Física d'Altes Energies (IFAE), Barcelona Institute of Science and Technology, Barcelona, Spain

[14] [(a)]Institute of High Energy Physics, Chinese Academy of Sciences, Beijing, China; [(b)]Physics Department, Tsinghua University, Beijing, China; [(c)]Department of Physics, Nanjing University, Nanjing, China; [(d)]University of Chinese Academy of Science (UCAS), Beijing, China
[15] Institute of Physics, University of Belgrade, Belgrade, Serbia
[16] Department for Physics and Technology, University of Bergen, Bergen, Norway
[17] [(a)]Physics Division, Lawrence Berkeley National Laboratory, Berkeley, CA, USA; [(b)]University of California, Berkeley, CA, USA
[18] Institut für Physik, Humboldt Universität zu Berlin, Berlin, Germany
[19] Albert Einstein Center for Fundamental Physics and Laboratory for High Energy Physics, University of Bern, Bern, Switzerland
[20] School of Physics and Astronomy, University of Birmingham, Birmingham, UK
[21] [(a)]Department of Physics, Bogazici University, Istanbul, Türkiye; [(b)]Department of Physics Engineering, Gaziantep University, Gaziantep, Türkiye; [(c)]Department of Physics, Istanbul University, Istanbul, Türkiye; [(d)]Istinye University, Sariyer, Istanbul, Türkiye
[22] [(a)]Facultad de Ciencias y Centro de Investigaciónes, Universidad Antonio Nariño, Bogotá, Colombia; [(b)]Departamento de Física, Universidad Nacional de Colombia, Bogotá, Colombia
[23] [(a)]Dipartimento di Fisica e Astronomia A. Righi, Universitá di Bologna, Bologna, Italy; [(b)]INFN Sezione di Bologna, Bologna, Italy
[24] Physikalisches Institut, Universität Bonn, Bonn, Germany
[25] Department of Physics, Boston University, Boston, MA, USA
[26] Department of Physics, Brandeis University, Waltham, MA, USA
[27] [(a)]Transilvania University of Brasov, Brasov, Romania; [(b)]Horia Hulubei National Institute of Physics and Nuclear Engineering, Bucharest, Romania; [(c)]Department of Physics, Alexandru Ioan Cuza University of Iasi, Iasi, Romania; [(d)]Physics Department, National Institute for Research and Development of Isotopic and Molecular Technologies, Cluj-Napoca, Romania; [(e)]University Politehnica Bucharest, Bucharest, Romania; [(f)]West University in Timisoara, Timisoara, Romania; [(g)]Faculty of Physics, University of Bucharest, Bucharest, Romania
[28] [(a)]Faculty of Mathematics, Physics and Informatics, Comenius University, Bratislava, Slovak Republic; [(b)]Department of Subnuclear Physics, Institute of Experimental Physics of the Slovak Academy of Sciences, Kosice, Slovak Republic
[29] Physics Department, Brookhaven National Laboratory, Upton, NY, USA
[30] Departamento de Física, y CONICET, Facultad de Ciencias Exactas y Naturales, Instituto de Física de Buenos Aires (IFIBA), Universidad de Buenos Aires, Buenos Aires, Argentina
[31] California State University, Long Beach, CA, USA
[32] Cavendish Laboratory, University of Cambridge, Cambridge, UK
[33] [(a)]Department of Physics, University of Cape Town, Cape Town, South Africa; [(b)]iThemba Labs, Western Cape, South Africa; [(c)]Department of Mechanical Engineering Science, University of Johannesburg, Johannesburg, South Africa; [(d)]National Institute of Physics, University of the Philippines, Diliman, Philippines; [(e)]Department of Physics, University of South Africa, Pretoria, South Africa; [(f)]University of Zululand, KwaDlangezwa, South Africa; [(g)]School of Physics, University of the Witwatersrand, Johannesburg, South Africa
[34] Department of Physics, Carleton University, Ottawa, ON, Canada
[35] [(a)]Faculté des Sciences Ain Chock, Réseau Universitaire de Physique des Hautes Energies-Université Hassan II, Casablanca, Morocco; [(b)]Faculté des Sciences, Université Ibn-Tofail, Kénitra, Morocco; [(c)]Faculté des Sciences Semlalia, Université Cadi Ayyad, LPHEA-Marrakech, Morocco; [(d)]LPMR, Faculté des Sciences, Université Mohamed Premier, Oujda, Morocco; [(e)]Faculté des sciences, Université Mohammed V, Rabat, Morocco; [(f)]Institute of Applied Physics, Mohammed VI Polytechnic University, Ben Guerir, Morocco
[36] CERN, Geneva, Switzerland
[37] Affiliated with an institute covered by a cooperation agreement with CERN, Geneva, Switzerland
[38] Affiliated with an international laboratory covered by a cooperation agreement with CERN, Geneva, Switzerland
[39] Enrico Fermi Institute, University of Chicago, Chicago, IL, USA
[40] LPC, Université Clermont Auvergne, CNRS/IN2P3, Clermont-Ferrand, France
[41] Nevis Laboratory, Columbia University, Irvington, NY, USA
[42] Niels Bohr Institute, University of Copenhagen, Copenhagen, Denmark

[43] [(a)]Dipartimento di Fisica, Università della Calabria, Rende, Italy; [(b)]INFN Gruppo Collegato di Cosenza, Laboratori Nazionali di Frascati, Frascati, Italy
[44] Physics Department, Southern Methodist University, Dallas, TX, USA
[45] Physics Department, University of Texas at Dallas, Richardson, TX, USA
[46] National Centre for Scientific Research "Demokritos", Agia Paraskevi, Greece
[47] [(a)]Department of Physics, Stockholm University, Stockholm, Sweden; [(b)]Oskar Klein Centre, Stockholm, Sweden
[48] Deutsches Elektronen-Synchrotron DESY, Hamburg and Zeuthen, Germany
[49] Fakultät Physik , Technische Universität Dortmund, Dortmund, Germany
[50] Institut für Kern- und Teilchenphysik, Technische Universität Dresden, Dresden, Germany
[51] Department of Physics, Duke University, Durham, NC, USA
[52] SUPA-School of Physics and Astronomy, University of Edinburgh, Edinburgh, UK
[53] INFN e Laboratori Nazionali di Frascati, Frascati, Italy
[54] Physikalisches Institut, Albert-Ludwigs-Universität Freiburg, Freiburg, Germany
[55] II. Physikalisches Institut, Georg-August-Universität Göttingen, Göttingen, Germany
[56] Département de Physique Nucléaire et Corpusculaire, Université de Genève, Geneva, Switzerland
[57] [(a)]Dipartimento di Fisica, Università di Genova, Genoa, Italy; [(b)]INFN Sezione di Genova, Genoa, Italy
[58] II. Physikalisches Institut, Justus-Liebig-Universität Giessen, Giessen, Germany
[59] SUPA-School of Physics and Astronomy, University of Glasgow, Glasgow, UK
[60] LPSC, Université Grenoble Alpes, CNRS/IN2P3, Grenoble INP, Grenoble, France
[61] Laboratory for Particle Physics and Cosmology, Harvard University, Cambridge, MA, USA
[62] [(a)]Department of Modern Physics and State Key Laboratory of Particle Detection and Electronics, University of Science and Technology of China, Hefei, China; [(b)]Institute of Frontier and Interdisciplinary Science and Key Laboratory of Particle Physics and Particle Irradiation (MOE), Shandong University, Qingdao, China; [(c)]School of Physics and Astronomy, Shanghai Jiao Tong University, Key Laboratory for Particle Astrophysics and Cosmology (MOE), SKLPPC, Shanghai, China; [(d)]Tsung-Dao Lee Institute, Shanghai, China
[63] [(a)]Kirchhoff-Institut für Physik, Ruprecht-Karls-Universität Heidelberg, Heidelberg, Germany; [(b)]Physikalisches Institut, Ruprecht-Karls-Universität Heidelberg, Heidelberg, Germany
[64] [(a)]Department of Physics, Chinese University of Hong Kong, Shatin, N.T., Hong Kong, China; [(b)]Department of Physics, University of Hong Kong, Hong Kong, China; [(c)]Department of Physics and Institute for Advanced Study, Hong Kong University of Science and Technology, Clear Water Bay, Kowloon, Hong Kong, China
[65] Department of Physics, National Tsing Hua University, Hsinchu, Taiwan
[66] IJCLab, Université Paris-Saclay, CNRS/IN2P3, 91405 Orsay, France
[67] Department of Physics, Indiana University, Bloomington, IN, USA
[68] [(a)]INFN Gruppo Collegato di Udine, Sezione di Trieste, Udine, Italy; [(b)]ICTP, Trieste, Italy; [(c)]Dipartimento Politecnico di Ingegneria e Architettura, Università di Udine, Udine, Italy
[69] [(a)]INFN Sezione di Lecce, Lecce, Italy; [(b)]Dipartimento di Matematica e Fisica, Università del Salento, Lecce, Italy
[70] [(a)]INFN Sezione di Milano, Milan, Italy; [(b)]Dipartimento di Fisica, Università di Milano, Milan, Italy
[71] [(a)]INFN Sezione di Napoli, Naples, Italy; [(b)]Dipartimento di Fisica, Università di Napoli, Naples, Italy
[72] [(a)]INFN Sezione di Pavia, Pavia, Italy; [(b)]Dipartimento di Fisica, Università di Pavia, Pavia, Italy
[73] [(a)]INFN Sezione di Pisa, Pisa, Italy; [(b)]Dipartimento di Fisica E. Fermi, Università di Pisa, Pisa, Italy
[74] [(a)]INFN Sezione di Roma, Rome, Italy; [(b)]Dipartimento di Fisica, Sapienza Università di Roma, Rome, Italy
[75] [(a)]INFN Sezione di Roma Tor Vergata, Rome, Italy; [(b)]Dipartimento di Fisica, Università di Roma Tor Vergata, Rome, Italy
[76] [(a)]INFN Sezione di Roma Tre, Rome, Italy; [(b)]Dipartimento di Matematica e Fisica, Università Roma Tre, Rome, Italy
[77] [(a)]INFN-TIFPA, Povo, Italy; [(b)]Università degli Studi di Trento, Trento, Italy
[78] Department of Astro and Particle Physics, Universität Innsbruck, Innsbruck, Austria
[79] University of Iowa, Iowa City, IA, USA
[80] Department of Physics and Astronomy, Iowa State University, Ames, IA, USA
[81] [(a)]Departamento de Engenharia Elétrica, Universidade Federal de Juiz de Fora (UFJF), Juiz de Fora, Brazil; [(b)]Universidade Federal do Rio de Janeiro COPPE/EE/IF, Rio de Janeiro, Brazil; [(c)]Instituto de Física, Universidade de São Paulo, São Paulo, Brazil; [(d)]Rio de Janeiro State University, Rio de Janeiro, Brazil
[82] KEK, High Energy Accelerator Research Organization, Tsukuba, Japan
[83] Graduate School of Science, Kobe University, Kobe, Japan

[84] [(a)]Faculty of Physics and Applied Computer Science, AGH University of Science and Technology, Krakow, Poland; [(b)]Marian Smoluchowski Institute of Physics, Jagiellonian University, Krakow, Poland
[85] Institute of Nuclear Physics Polish Academy of Sciences, Krakow, Poland
[86] Faculty of Science, Kyoto University, Kyoto, Japan
[87] Kyoto University of Education, Kyoto, Japan
[88] Research Center for Advanced Particle Physics and Department of Physics, Kyushu University, Fukuoka , Japan
[89] Instituto de Física La Plata, Universidad Nacional de La Plata and CONICET, La Plata, Argentina
[90] Physics Department, Lancaster University, Lancaster, UK
[91] Oliver Lodge Laboratory, University of Liverpool, Liverpool, UK
[92] Department of Experimental Particle Physics, Jožef Stefan Institute and Department of Physics, University of Ljubljana, Ljubljana, Slovenia
[93] School of Physics and Astronomy, Queen Mary University of London, London, UK
[94] Department of Physics, Royal Holloway University of London, Egham, UK
[95] Department of Physics and Astronomy, University College London, London, UK
[96] Louisiana Tech University, Ruston, LA, USA
[97] Fysiska institutionen, Lunds universitet, Lund, Sweden
[98] Departamento de Física Teorica C-15 and CIAFF, Universidad Autónoma de Madrid, Madrid, Spain
[99] Institut für Physik, Universität Mainz, Mainz, Germany
[100] School of Physics and Astronomy, University of Manchester, Manchester, UK
[101] CPPM, Aix-Marseille Université, CNRS/IN2P3, Marseille, France
[102] Department of Physics, University of Massachusetts, Amherst, MA, USA
[103] Department of Physics, McGill University, Montreal, QC, Canada
[104] School of Physics, University of Melbourne, Victoria, Australia
[105] Department of Physics, University of Michigan, Ann Arbor, MI, USA
[106] Department of Physics and Astronomy, Michigan State University, East Lansing, MI, USA
[107] Group of Particle Physics, University of Montreal, Montreal, QC, Canada
[108] Fakultät für Physik, Ludwig-Maximilians-Universität München, Munich, Germany
[109] Max-Planck-Institut für Physik (Werner-Heisenberg-Institut), Munich, Germany
[110] Graduate School of Science and Kobayashi-Maskawa Institute, Nagoya University, Nagoya, Japan
[111] Department of Physics and Astronomy, University of New Mexico, Albuquerque, NM, USA
[112] Institute for Mathematics, Astrophysics and Particle Physics, Radboud University/Nikhef, Nijmegen, The Netherlands
[113] Nikhef National Institute for Subatomic Physics and University of Amsterdam, Amsterdam, The Netherlands
[114] Department of Physics, Northern Illinois University, DeKalb, IL, USA
[115] [(a)]New York University Abu Dhabi, Abu Dhabi, United Arab Emirates; [(b)]University of Sharjah, Sharjah, United Arab Emirates
[116] Department of Physics, New York University, New York, NY, USA
[117] Ochanomizu University, Otsuka, Bunkyo-ku, Tokyo, Japan
[118] Ohio State University, Columbus, OH, USA
[119] Homer L. Dodge Department of Physics and Astronomy, University of Oklahoma, Norman, OK, USA
[120] Department of Physics, Oklahoma State University, Stillwater, OK, USA
[121] Palacký University, Joint Laboratory of Optics, Olomouc, Czech Republic
[122] Institute for Fundamental Science, University of Oregon, Eugene, OR, USA
[123] Graduate School of Science, Osaka University, Osaka, Japan
[124] Department of Physics, University of Oslo, Oslo, Norway
[125] Department of Physics, Oxford University, Oxford, UK
[126] LPNHE, Sorbonne Université, Université Paris Cité, CNRS/IN2P3, Paris, France
[127] Department of Physics, University of Pennsylvania, Philadelphia, PA, USA
[128] Department of Physics and Astronomy, University of Pittsburgh, Pittsburgh, PA, USA
[129] [(a)]Laboratório de Instrumentação e Física Experimental de Partículas-LIP, Lisbon, Portugal; [(b)]Departamento de Física, Faculdade de Ciências, Universidade de Lisboa, Lisbon, Portugal; [(c)]Departamento de Física, Universidade de Coimbra, Coimbra, Portugal; [(d)]Centro de Física Nuclear da Universidade de Lisboa, Lisbon, Portugal; [(e)]Departamento de Física, Universidade do Minho, Braga, Portugal; [(f)]Departamento de Física Teórica y del Cosmos, Universidad de Granada, Granada, Spain; [(g)]Departamento de Física, Instituto Superior Técnico, Universidade de Lisboa, Lisbon, Portugal

[130] Institute of Physics of the Czech Academy of Sciences, Prague, Czech Republic
[131] Czech Technical University in Prague, Prague, Czech Republic
[132] Faculty of Mathematics and Physics, Charles University, Prague, Czech Republic
[133] Particle Physics Department, Rutherford Appleton Laboratory, Didcot, UK
[134] IRFU, CEA, Université Paris-Saclay, Gif-sur-Yvette, France
[135] Santa Cruz Institute for Particle Physics, University of California Santa Cruz, Santa Cruz, CA, USA
[136] [(a)]Departamento de Física, Pontificia Universidad Católica de Chile, Santiago, Chile; [(b)]Millennium Institute for Subatomic Physics at High Energy Frontier (SAPHIR), Santiago, Chile; [(c)]Instituto de Investigación Multidisciplinario en Ciencia y Tecnología y Departamento de Física, Universidad de La Serena, La Serena, Chile; [(d)]Department of Physics, Universidad Andres Bello, Santiago, Chile; [(e)]Instituto de Alta Investigación, Universidad de Tarapacá, Arica, Chile; [(f)]Departamento de Física, Universidad Técnica Federico Santa María, Valparaíso, Chile
[137] Department of Physics, University of Washington, Seattle, WA, USA
[138] Department of Physics and Astronomy, University of Sheffield, Sheffield, UK
[139] Department of Physics, Shinshu University, Nagano, Japan
[140] Department Physik, Universität Siegen, Siegen, Germany
[141] Department of Physics, Simon Fraser University, Burnaby, BC, Canada
[142] SLAC National Accelerator Laboratory, Stanford, CA, USA
[143] Department of Physics, Royal Institute of Technology, Stockholm, Sweden
[144] Departments of Physics and Astronomy, Stony Brook University, Stony Brook, NY, USA
[145] Department of Physics and Astronomy, University of Sussex, Brighton, UK
[146] School of Physics, University of Sydney, Sydney, Australia
[147] Institute of Physics, Academia Sinica, Taipei, Taiwan
[148] [(a)]E. Andronikashvili Institute of Physics, Iv. Javakhishvili Tbilisi State University, Tbilisi, Georgia; [(b)]High Energy Physics Institute, Tbilisi State University, Tbilisi, Georgia; [(c)]University of Georgia, Tbilisi, Georgia
[149] Department of Physics, Technion, Israel Institute of Technology, Haifa, Israel
[150] Raymond and Beverly Sackler School of Physics and Astronomy, Tel Aviv University, Tel Aviv, Israel
[151] Department of Physics, Aristotle University of Thessaloniki, Thessaloniki, Greece
[152] International Center for Elementary Particle Physics and Department of Physics, University of Tokyo, Tokyo, Japan
[153] Department of Physics, Tokyo Institute of Technology, Tokyo, Japan
[154] Department of Physics, University of Toronto, Toronto, ON, Canada
[155] [(a)]TRIUMF, Vancouver, BC, Canada; [(b)]Department of Physics and Astronomy, York University, Toronto, ON, Canada
[156] Division of Physics and Tomonaga Center for the History of the Universe, Faculty of Pure and Applied Sciences, University of Tsukuba, Tsukuba, Japan
[157] Department of Physics and Astronomy, Tufts University, Medford, MA, USA
[158] United Arab Emirates University, Al Ain, United Arab Emirates
[159] Department of Physics and Astronomy, University of California Irvine, Irvine, CA, USA
[160] Department of Physics and Astronomy, University of Uppsala, Uppsala, Sweden
[161] Department of Physics, University of Illinois, Urbana, IL, USA
[162] Instituto de Física Corpuscular (IFIC), Centro Mixto Universidad de Valencia-CSIC, Valencia, Spain
[163] Department of Physics, University of British Columbia, Vancouver, BC, Canada
[164] Department of Physics and Astronomy, University of Victoria, Victoria, BC, Canada
[165] Fakultät für Physik und Astronomie, Julius-Maximilians-Universität Würzburg, Würzburg, Germany
[166] Department of Physics, University of Warwick, Coventry, UK
[167] Waseda University, Tokyo, Japan
[168] Department of Particle Physics and Astrophysics, Weizmann Institute of Science, Rehovot, Israel
[169] Department of Physics, University of Wisconsin, Madison, WI, USA
[170] Fakultät für Mathematik und Naturwissenschaften, Fachgruppe Physik, Bergische Universität Wuppertal, Wuppertal, Germany
[171] Department of Physics, Yale University, New Haven, CT, USA

[a] Also Affiliated with an institute covered by a cooperation agreement with CERN, Geneva, Switzerland
[b] Also at Borough of Manhattan Community College, City University of New York, New York, NY, USA
[c] Also at Bruno Kessler Foundation, Trento, Italy

[d] Also at Center for High Energy Physics, Peking University, Beijing, China
[e] Also at Centro Studi e Ricerche Enrico Fermi, Rome, Italy
[f] Also at CERN, Geneva, Switzerland
[g] Also at Département de Physique Nucléaire et Corpusculaire, Université de Genève, Geneva, Switzerland
[h] Also at Departament de Fisica de la Universitat Autonoma de Barcelona, Barcelona, Spain
[i] Also at Department of Financial and Management Engineering, University of the Aegean, Chios, Greece
[j] Also at Department of Physics and Astronomy, Michigan State University, East Lansing, MI, USA
[k] Also at Department of Physics and Astronomy, University of Louisville, Louisville, KY, USA
[l] Also at Department of Physics, Ben Gurion University of the Negev, Beer Sheva, Israel
[m] Also at Department of Physics, California State University, East Bay, USA
[n] Also at Department of Physics, California State University, Sacramento, USA
[o] Also at Department of Physics, King's College London, London, UK
[p] Also at Department of Physics, University of Fribourg, Fribourg, Switzerland
[q] Also at Department of Physics, University of Thessaly, Thessaly, Greece
[r] Also at Department of Physics, Westmont College, Santa Barbara, USA
[s] Also at Hellenic Open University, Patras, Greece
[t] Also at Institucio Catalana de Recerca i Estudis Avancats, ICREA, Barcelona, Spain
[u] Also at Institut für Experimentalphysik, Universität Hamburg, Hamburg, Germany
[v] Also at Institute of Particle Physics (IPP), Toronto, Canada
[w] Also at Institute of Physics, Azerbaijan Academy of Sciences, Baku, Azerbaijan
[x] Also at Institute of Theoretical Physics, Ilia State University, Tbilisi, Georgia
[y] Also at Lawrence Livermore National Laboratory, Livermore, USA
[z] Also at The Collaborative Innovation Center of Quantum Matter (CICQM), Beijing, China
[aa] Also at TRIUMF, Vancouver, BC, Canada
[ab] Also at Università di Napoli Parthenope, Naples, Italy
[ac] Also at University of Chinese Academy of Sciences (UCAS), Beijing, China
[ad] Also at Department of Physics, University of Colorado Boulder, Colorado, USA
[ae] Also at Washington College, Chestertown, MD, USA
[af] Also at Yeditepe University, Physics Department, Istanbul, Türkiye
[ag] Also at Physics Department, An-Najah National University, Nablus, Palestine
[*] Deceased